Supplementary material

Molecular targets for endogenous GDNF modulation in striatal parvalbumin interneurons

Daniel Enterría-Morales, Natalia Lopez-Gonzalez del Rey, Javier Blesa, Ivette López-López, Sarah Gallet, Vincent Prévot, José López-Barneo, Xavier d'Anglemont de Tassigny.

Content:

- Supplementary material and methods
- Supplementary figures 1 to 11
- Supplementary references
- Supplementary tables 1 to 5

Supplementary material and methods

Mouse genotyping

Routine genotyping to detect *Gdnf*^{LacZ}, *PV-Cre*, *tdTomato* or *ChR2-tdTomato* alleles was performed by PCR.

- *Gdnf*^{LacZ} was detected with the following primers:

BH122 (5'-GGAGGGAGCGGTTCTTACAG-3')
BH129 (5'-CTTGCCTGGTGCGGTTCT CT-3')
BH128 (5'-GCTGGCGAAAGGGGGATGTG-3')

- *PV-Cre* PCR was performed with the primers:

CreFW (5'- TGTTCAGGGATCGCCAG -3')
CreREV (5'-ACGGGCACTGTGTCCAG-3')

- *tdTomato* allele was detected with:

dTomFW (5'- ACTGCAGCGCTGGTCATATG -3')
dTomREV (5'- ACTCTTTGATGACCTCCTCG -3')

- The presence of the *ChR2-tdTomato* allele was verified by using:

ChR2FW (5'- GGCATTAAAGCAGCGTATCC -3')
ChR2REV (5'- CTGTTCCTGTACGGCATGG -3')

Histological and immunohistochemical procedures

For histological and immunohistochemical analyses on mice, 2-month-old male mouse brain sections were prepared as follows. Mice were deeply anesthetized by intraperitoneal injection of thiobarbital and intracardially perfused with phosphate-buffered saline 0.1M (PBS) followed by 4% paraformaldehyde in PBS pH 7.4. After a 1-hour post-fixation step, brains were washed in PBS, cryoprotected in PBS with 30% sucrose, embedded in Tissue-Tek® O.C.T. Compound (Sakura®, Finetek), and frozen on dry ice. Coronal floating sections (30 µm thick) were obtained throughout the striatum and somatosensory and motor cortex using a cryostat (CM 1950, Leica Biosystems). Sections were stored at -20°C in an antifreeze solution (0.9% w/v NaCl, 30% w/v sucrose, 1% w/v Polyvinylpyrrolidone (9003-39-8, Sigma), 30% v/v Ethylene glycol in PBS) until use.

For PV and cKit co-labelling in mouse brain sections, monoclonal mouse anti-PV antibody (PV235, Swant, Switzerland) at 1:4000 was combined with anti c-Kit (D13A2) XP® rabbit monoclonal Antibody (Cell Signaling Technology, The Netherlands) at 1:1000 dilution. Both anti-PV and anti-cKit primary antibodies have been previously used by us (Enterría-Morales *et al.*, 2016), and others (Chen *et al.*, 2017; Abreu *et al.*, 2018). Primary and secondary antibodies were prepared in PBS with 0.1% Triton X-100 (PBST), 10% fetal bovine serum and 1 mg/ml bovine serum albumin (Sigma). Sections were incubated with primary antibodies overnight at 4°C, and then incubated with secondary anti-IgG antibodies conjugated with either Alexa Fluor 488 or 568 (Invitrogen) for 1 hour at room temperature. Nuclei were labelled with 4',6'-diamidino-2-phenylindole (Dapi, D9542, Sigma). Immunofluorescent images were obtained with a BX61 microscope equipped with a DP70 camera (Olympus), or a N-STORM super-resolution microscope system (Nikon) equipped with 405 / 488 / 561 / 647 nm lasers.

For histological detection of GDNF expression, β-galactosidase activity was revealed with 5-bromo-4-chloro-3-indolyl- β-D-galactopyranoside (XGal) staining (Hidalgo-Figueroa *et al.*, 2012). Briefly, coronal brain floating sections (40 µm-thick) from adult heterozygous $Gdnf^{LacZ}$ mice were incubated with XGal solution for 16 hours at room temperature (RT) and then washed with PBS 0.1M. For colocalization study, we performed immunohistochemistry as described above. Primary anti-PV antibody (PV27, Swant, Switzerland) was diluted at 1:4000, and secondary anti-rabbit IgG antibody was conjugated to horseradish peroxidase (HRP) and revealed as a light brown precipitate by 3,3'-Diaminobenzidine (DAB) reaction (d'Anglemont de Tassigny *et al.*, 2010).

For immunofluorescence PV and cKit double-staining of monkey (*Macaca fascicularis*) striatum, free-floating sections (40 µm thick) were incubated in sodium citrate buffer 10 mM for 30 min at 37ºC for antigen retrieval. Sections were rinsed 3 times for 5 min in 0.1 M TB and 3 times for 5 min in TBS, and maintained in a blocking solution containing 10% of normal rabbit serum (NRS)/0.4% Triton X-100 (TX) in TBS for 3 hours. Sections were incubated with primary antibody solutions containing mouse anti-PV (1:2500) (PV235, Swant) and goat anti-cKit (1:50) (AF332-SP, Thermo Fisher) in 4% NRS/0.2% Tx-TBS for 48 hours at 4°C. After primary incubation, the sections were rinsed 4 times for 5 min in TBS, and then incubated for 2 hours in the secondary antibody solution containing Alexa Fluor rabbit anti-mouse 488 (1:100) (A-11059) and Alexa Fluor rabbit anti-goat 568 (1:100) (A-11079) in 4% NRS/0.2Tx-TBS. After 2 × 5 min rinses in TBS the sections were mounted onto glass slides.

For single detection of PV interneurons, same conditions were applied as above with the difference that the secondary antibody was a biotinylated rabbit anti-mouse (1:400) (AP160B, Millipore) and the sections were incubated in Vectastain Elite avidin/biotin complex from Vector Labs (Burligame, CA) prior to peroxidase development. A standard diaminobenzidine protocol (0.05% diaminobenzidine and 0.003% H_2O_2) was used.

Immunohistochemical analyses

To determine the degree of co-expression between PV and cKit in the mouse striatum, photographs of PV and cKit fluorescent staining were acquired separately with the 20X objective from a BX61 Olympus microscope and merged with Photoshop CC (Adobe) for dual-labelled cells analysis. Five fields in the dorsomedial region of the striatum were analysed per animal (N = 3). PV and cKit single cells and PV / cKit double labelled cells were counted.

The density of PV-positive cells in the striatum of normal and MPTP monkeys was estimated by using an unbiased stereological approach. Seven rostro-caudal sections, regularly spaced at intervals of 2400 µm, were examined for each monkey. Three sections were rostral and four sections caudal to the level where the anterior commissure crosses the midline. All measurements were performed using an interactive computer system consisting of a Zeiss Axioskop optical microscope (Oberkochen, Germany) equipped with a digital camera (AxioCam HRc, Zeiss, Germany). The interactive test grids and the motorized stage were controlled by Stereo Investigator software (version 8.0, MicroBrightField, Williston, VT, USA). The contours of the striatum were first outlined at a low magnification (2X) and neurons were systematically sampled using a 40X lens. The results were expressed as the number of PV+ neurons per 100 mm^2.

Co-expression of PV and cKit was quantified in striatum (caudate nucleus and putamen separately) and cortex. Photographs of PV and cKit fluorescent staining were acquired separately with the 10X objective from a DM2500 microscope equipped with LAS V4.6 software (Leica) and merged for dual labelling analysis. Four fields per region and per animal (N = 3 or 4) were analysed. PV and cKit single cells and PV / cKit double-labelled cells were counted.

Tissue dissociation and cell preparation

Mice were sacrificed at P30 by thiobarbital overdose, and intracardially perfused with ice-cold oxygenated working solution (ICOWS; 87 mM NaCl, 2.5 mM KCl, 1.25 mM NaH_2PO4, 26 mM $NaHCO_3$, 75 mM sucrose, 20 mM glucose, 1 mM $CaCl_2$, and 2 mM $MgCl_2$). The brain was quickly dissected and transferred to ICOWS and kept in the same solution during sectioning on a vibratome (VT1200S, Leica Biosystems) in 300 µm-thick slices (Bregma, AP: +1.34 to −1.82 mm). The slices were placed in oxygenated working solution at 37°C for 45 minutes. The area of interest was then dissected from each slice, and the tissue was dissociated using the Papain dissociation system (Worthington Biochem), following the manufacturer's instructions. Solutions were saturated with carbogen (5% CO_2 / 95% O_2, Air Liquide) before use. Oxygenation and a short dissection time were crucial to maintain a high rate of cell survival. Next, the cell suspension was filtered through a 20 µm mesh (Bio-Fil) and kept in ICOWS with 0.2% bovine serum albumin prior to FACS immediately thereafter.

RNA preparation, quality control and quantitation

Total RNA from cortical and striatal whole tissue samples was isolated using TRIzol method (Thermo Fisher) following the manufacturer's guideline. For the FACS-sorted PV interneurons, *RNAlater* solution was first removed after a 1 min centrifugation at 5000 x g and cells were lysed in 0.5 ml TRIzol reagent. To improve the yield, an additional step was performed by incubating the upper aqueous phase obtained after chloroform-induced gradient with 0.5 µg glycogen (SERVA, Germany) at 4°C for 12 hrs. RNA quantity and quality check from the FACS sorted tdTomato-positive cells was performed with an Agilent 2100 Bioanalyzer system. Samples with RNA integrity number (RIN) ≥ 7 were further processed for microarray analysis. The yield and integrity of the RNA from the whole tissue sample was determined with the A_{260}/A_{280} ratio with a Nanodrop 2000 spectrophotometer (Thermo Fisher).

Real-time quantitative RT-PCR (qPCR)

Equal quantity (0.8 µg) of amplified RNA from PV cells or RNA from cortex and striatum tissue samples were copied to cDNA using the QuantiTect Reverse Transcription Kit (Qiagen) in a final volume of 100 µl. PCR reactions were performed in duplicate, each in a total volume of 20 µl containing 1 µl of cDNA, 10 µl SYBR Green Fast Mix

(Thermo Fisher), 1 µl FW primer, 1 µl REV primer and 7 µl H_2O. Real-time quantitative PCR reactions were performed in a 7500 Fast Real Time PCR System (Life Technologies). *Actb* gene expression was used to normalize the amount of RNA inputs and perform relative quantifications (ΔΔCt method). The primers used to amplify the cDNA samples are listed in Supplementary Table 1. Primer specificity and sensitivity was tested for each set of primers prior to use.

For *ex vivo* experiments, we used TaqMan probes to measure variations of gene expression (Thermo Fisher) for *Gdnf* (Mm00599849_m1) and *Fos* (Mm00487425_m1), with *Hmbs* (Mm00660262_g1) and *Actb* (Mm01205647_g1) as internal control respectively. The *Pvalb* probe (Mm00443100_m1) was also used for post-FACS gene expression.

RNAscope

We carried out *in situ* hybridization using the protocol from Advanced Cell Diagnostics (ACDbio), following the manufacturer's guidelines (Cat. No. 320851, RNAscope® Fluorescent Multiplex kit). To minimize the degradation of the RNA, we worked under a sterile environment, cleaning all the material with EtOH 70% and RNaseZap™ (Thermo Fisher) before use. In addition, we prepared all the solutions in Diethyl pyrocarbonate (DEPC, Sigma) treated water (DEPC-H_2O). We used 4-month-old wild-type mice that were euthanized by decapitation under isofluorane (Sigma) anesthesia. Isoflurane does not alter gene expression. The brain was quickly extracted, placed in OCT (Tissue-Tek) and rapidly frozen by dry ice-cooled isopentane. Frozen block was stored at -80 ºC until cryo-sectioning. 18-µm thick sections (+1.34 to −1.82 mm from Bregma) were mounted onto SuperFrost Plus Slides (Thermo Fisher), then fixed with PFA 4% for 15 minutes at 4 ºC, and washed 3 times with PBS 0.1M. Next, tissue was dehydrated in ethanol 50%, 70% and 100%. For hybridization protocol, we followed the manufacturer's guideline and reagents. Briefly, the tissue was treated with Protease IV to permeabilize and retrieve RNA, and then we used probes for mouse *Gdnf* (cat. No. 421951), *Lhx8* (cat. No. 515101-C2) and *Gpr83* (cat. No. 317431-C3) designed by ACDBio. The probes were first activated for 10 minutes at 40 ºC in the HybEZTM Oven (ACDBio), and then added to the tissue to hybridize the RNA of interest for 2 hours at 40 ºC, one probe at a time. After hybridization, the tissue was washed and incubated with amplifiers in the following order: Amp1-FL for 30 minutes at 40 ºC, Amp2-FL for 15 minutes at 40 ºC and Amp3-FL for 30 minutes at 40 ºC, and Amp4-FL Alt B for 15 minutes at 40 ºC. The Amp4-FL Alt B reagent contains the fluorophores Atto 550, Alexa 488 and Atto 647, allowing the detection of single molecules of mRNA for *Gdnf* (red), *Lhx8* (green), and *Gpr83* (magenta). Finally, the samples were incubated with DAPI (ACDBio) to stain the nuclei, and mounted with Fluorescence Mounting Medium (Sigma). The slides were stored at 4 ºC until microscope analysis. We used negative and positive probes to test the protocol. The positive probe hybridized with mouse *Ubc* mRNA, and the negative probe hybridized with bacterial *DapB* mRNA (both provided by ACDBio).

We analysed microphotographs taken at three different striatal slices from three different mice. To quantify the cells expressing *Gdnf*, *Lhx8* and *Gpr83* mRNA, the number of *Gdnf*-positive cells, *Lhx8*-positive cells, *Gpr83*-positive cells, and double positive cells (*Gdnf*+/*Lhx8*+, *Gdnf*+/*Gpr83*+, *Lhx8*+/*Gpr83*+) was manually counted in 3-4 dorsolateral striatal fields and reported as the number of positive cells per square millimeter (mm^2), knowing that each field measured 0.296 mm^2. Data are represented as the percentage of *Gdnf*-positive cells expressing *Lhx8* and *Gpr83*, the percentage of *Gdnf*-positive cells expressing *Lhx8*, the percentage of *Gdnf*-positive cells expressing *Gpr83*, and the percentage of *Lhx8*-positive cells expressing *Gpr83*.

Ex vivo pharmacological experiments

P30 male mice were deeply anesthetized by i.p. injection of thiobarbital and intracardially perfused with ice-cold cutting solution (ICS) (sucrose 222mM, glucose 11mM, KCl 3mM, NaH_2PO_4 1mM, $NaHCO_3$ 26mM, $MgCl_2$ 7mM, $CaCl_2$ 0.5mM) saturated with 95% O_2 / 5% CO_2 mixture. Once perfused, the brain was rapidly removed, placed in ICS and cut in 250µm-thick coronal slices containing the striatum using an anti-vibration device-equipped VT1200S vibratome (Leica). Slices were split in two halves (hemispheres) and placed in artificial cerebrospinal fluid (aCSF) (sucrose 4 mM, glucose 10 mM, KCl 2.5 mM, NaH_2PO_4 1.25 mM, $NaHCO_3$ 26 mM, $MgCl_2$ 1 mM, $CaCl_2$ 2.5 mM and NaCl 124 mM). aCSF was continuously bubbled with 95% O_2 / 5% CO_2 to reach physiological pH values at 36°C. After a 30 min acclimatization period, aCSF was changed for a pre-warmed oxygenized aCSF with different pharmacological drugs (or vehicle control) and slices were incubated for up to twelve hours. After a first series of tests, the optimal *ex vivo* incubation time was set to 5 hours. When incubation time was up, striatal tissue was cut out from the slices and placed in *RNAlater* (for RNA), then stored at -80 °C.

For *ex vivo* experimental validation, viability of striatal slices was checked by measuring high-K^+-induced (40 mM) catecholamine release by amperometry (Urena *et al.*, 1994; Mejías *et al.*, 2006). Recordings were done after up to 12 hours of incubation time with a polarized carbon fibre electrode placed in the dorso-medial part of the striatum under microscope control. Pharmacological drugs and selected GPCR agonists tested were: dibutyryl cyclic AMP (D0627, Sigma), forskolin (F6886, Sigma), 666-15 (5661, Tocris), $CdCl_2$ (Sigma), mPEN (004-58, Phoenix Europe, Germany), melanotan II (2566, Tocris), Senktide (1068, Tocris), GR73632 (1669, Tocris).

In vivo stereotaxic experiments

Two-month-old wild-type male mice were anesthetized with ketamine and xylazine dosage according to the Cold Spring Harbor Protocols 2006 and immobilized on a stereotaxic device (Stoelting). Each mouse received a bilateral intrastriatal injection (1 or 2 µL) of 49 µg dibutyryl cyclic AMP, 8.2 µg forskolin or vehicle (PBS or DMSO respectively) through a 30-gauge Hamilton syringe, with positive pressure on. The stereotaxic coordinates for the injection site in the dorsomedial striatum ventricle were +0.5 mm anteroposterior, 1.8 mm lateral to the bregma and −3.0 mm from the skull surface according to the Paxinos mouse brain atlas (Paxinos and Franklin, 2001). The syringe was kept in place for 5 min after each injection. Animals were next placed to recover in a warmed box, and were euthanatized 4 hours after the second injection by thiobarbital overdose. Striata were separately removed, snap frozen and kept at -80 ºC until RNA extraction as described above.

Supplementary Figure 1

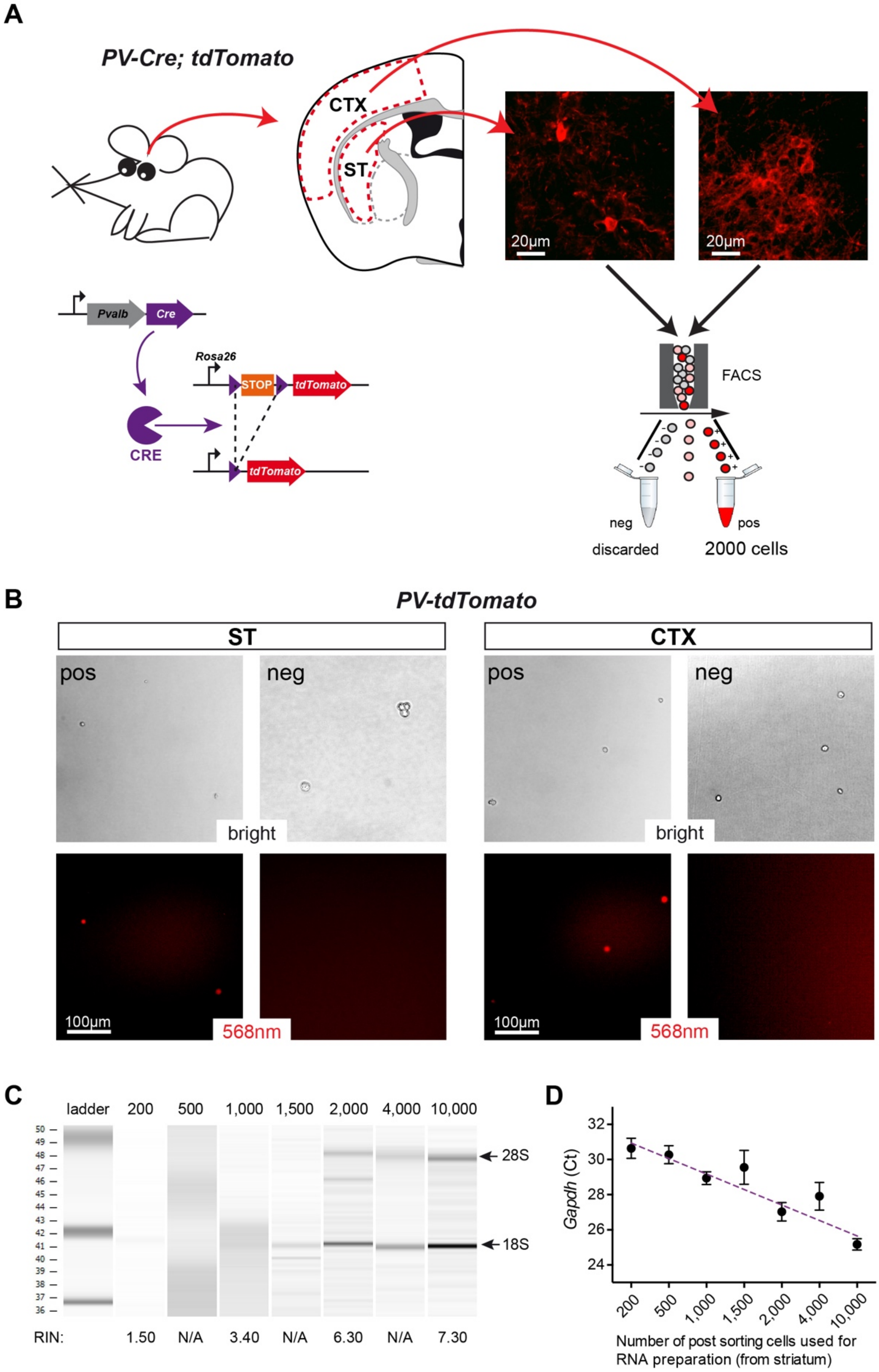

Supplementary figure 1. Experimental workflow for cell sorting from *PV-Cre;tdTomato* mice and quality tests on post-FACS cells and RNA. (**A**) Left, gene construction of *PV-Cre;tdTomato* mice and schematic illustration of cortex (CTX) and striatum (ST) tissue samples obtained for cell dispersion. The reporter strategy is based on tdTomato reporter gene expression after deletion of floxed-STOP codon by Cre recombinase expressed under the *Pvalb* promoter. The *PV-Cre;tdTomato* model harbors an IRES-Cre-pA insert in the 3' UTR of exon 5 of the *Pvalb* gene, and carries a targeted transgene Channelrhodopsin-2/tdTomato fusion sequence preceded by a loxP-flanked STOP cassette in a *Rosa26* locus. CRE excision of the STOP signal results in expression of a ChR2/tdTomato fusion protein in the Cre-expressing PV neurons. Triangles indicate LoxP sites. Right, histological examples of fluorescent cells (tdTomato-positive) in cortex and striatum. tdTomato-positive cells were sorted by FACS (pos) and 2000 positive cells were pooled for further RNA extraction. (**B**) Phase contrast (upper row) and fluorescent (568 nm filter, lower row) microphotographs of floating FACS-captured striatal (ST) and cortical (CTX) cells from *PV-tdTomato* mice. This figure is complementary to figure 2 in the main article. (**C**) RNA quantity and quality check from increasing number of striatal cells captured after cytometry was performed to set the number of cells needed for microarray experiments. Arrows indicate the bands corresponding to 18S and 28S ribosomal RNA. The RNA integrity number (RIN) for each sample is indicated at the bottom of each line (N/A: not available). (**D**) Quantitative RT-PCR for a constitutive gene (*Gapdh*) indicates that the cycle threshold (Ct) is inversely proportional to the increasing number of post-FACS striatal cells harvested. Based on the results displayed in (C) and (D), the minimum number of PV+ cells used for post-FACS microarray analysis was set to 2,000.

Supplementary Figure 2

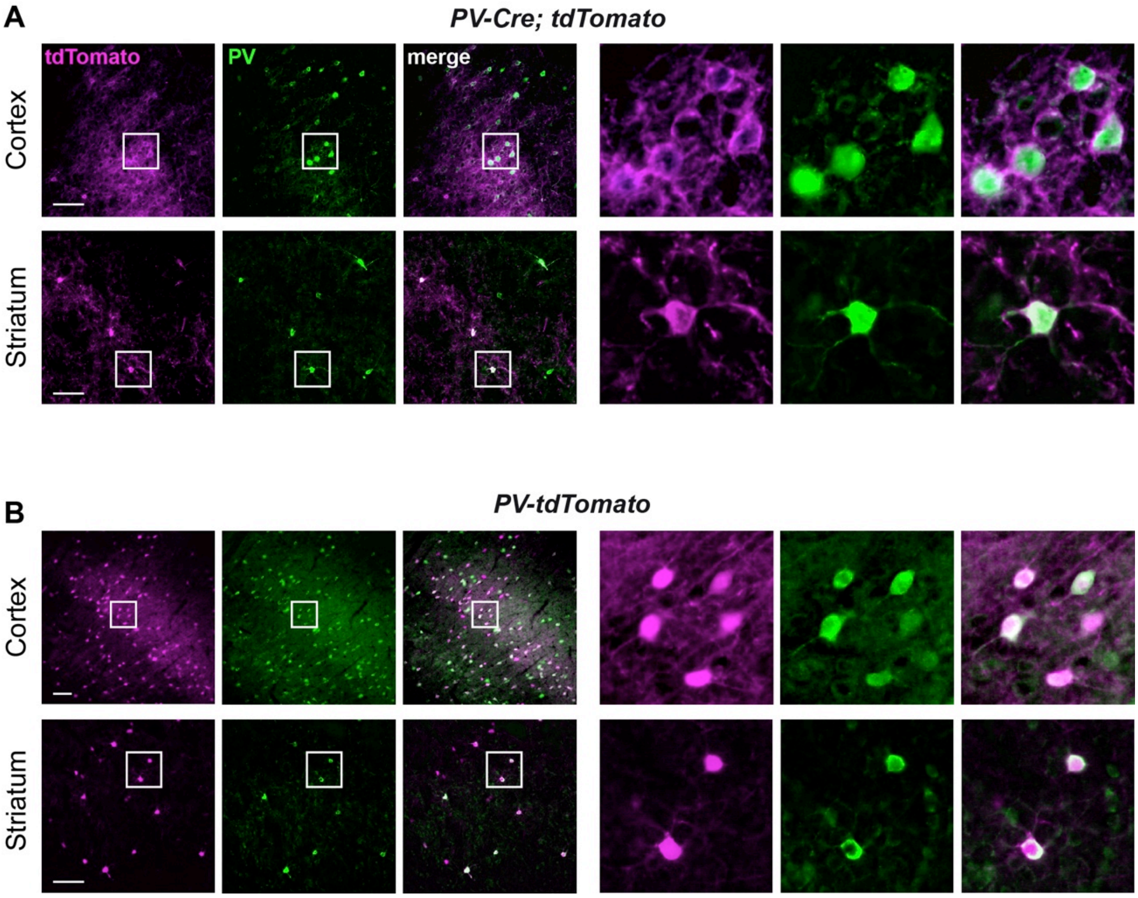

Supplementary figure 2. Expression of tdTomato reporter in parvalbumin interneurons. (**A**) Dual label microphotographs showing tdTomato-positive cells (magenta) and parvalbumin (PV) immunostained interneurons (green) in cortex or striatum from *PV-Cre;tdTomato* mice. Note the membrane-bound localization of tdTomato in the *PV-Cre;tdTomato* mice as a result of the ChR2/tdTomato fusion. See (Entería-Morales *et al.*, 2020) for co-labelled cells quantification in these mice. (**B**) Dual label microphotographs showing tdTomato-positive cells (magenta) and PV immunostained interneurons (green) in cortex or striatum from *PV-tdTomato* mice. Note the high degree of tdTomato and PV co-labelling in the cortex and striatum of *PV-tdTomato* mice. See Kaiser *et al.*, (2015) for co-labelling quantification in this model. Scale bars = 50 µm. Photos on right panels are magnified fields from lower magnification pictures on the left panels. This figure is complementary to figure 2 in the main article.

Supplementary Figure 3

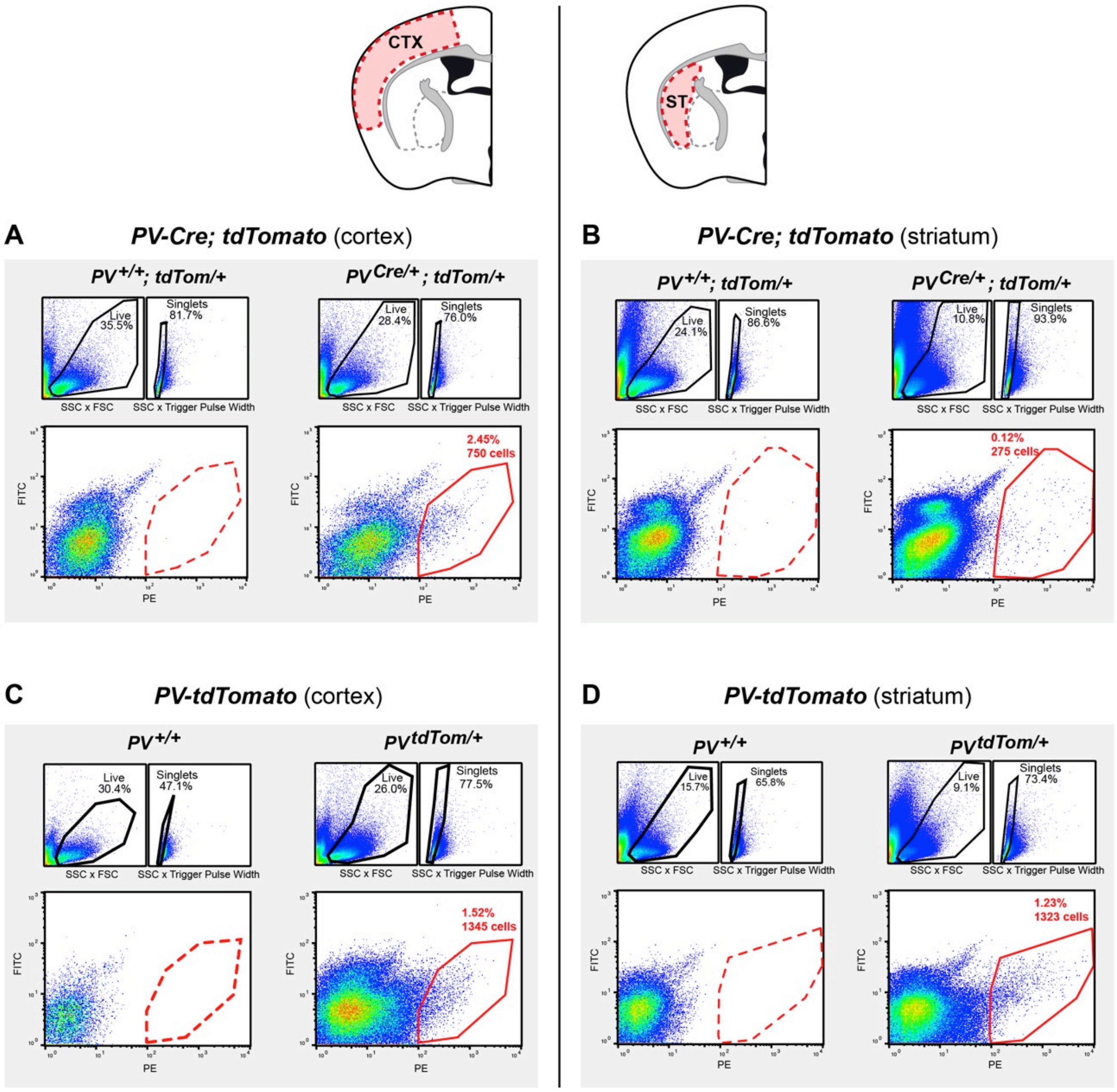

Supplementary figure 3. Flow cytometry graphical analysis of cells dispersed from cortex or striatum of tdTomato reporter mice. Top, schematic illustration of a coronal section of the mouse brain indicating the regions used for FACS (cortex, CTX; striatum, ST). (**A**) Illustrative plot from *PV-Cre;tdTomato* cortex. (**B**) Illustrative plot from *PV-Cre;tdTomato* striatum. (**C**) Illustrative plot from *PV-tdTomato* cortex. (**D**) Illustrative plot from *PV-tdTomato* striatum. In each experiment, relevant and living cells were selected with side scatter and forward scatter (SSC × FSC), then cell clumps were discarded by SSC × Trigger Pulse Width. The gates to isolate tdTomato-positive cells (red lines) were based on fluorescein isothiocyanate / phycoerythrin (FITC × PE) compensation to discard autofluorescence from tdTomato-negative animals of *PV*$^{+/+}$*;tdTom/+* or *PV*$^{+/+}$ genotypes (dotted red lines). The percentage and total number of tdTomato-positive cells harvested in each experiment are indicated in red. This figure is complementary to figure 2 in the main article.

Supplementary Figure 4

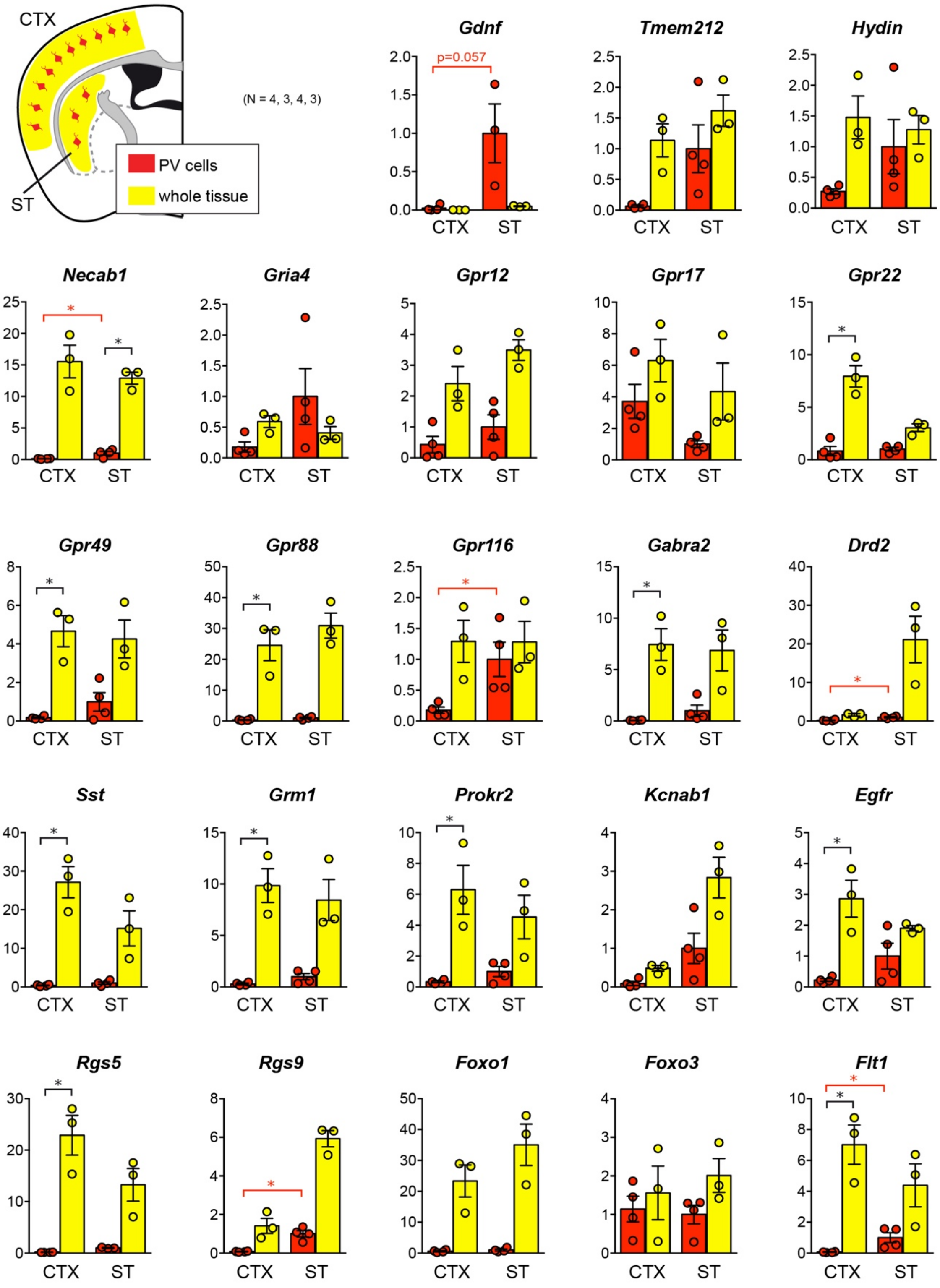

Supplementary figure 4. Differential gene expression between parvalbumin interneurons from striatum and cortex compared to tissue gene expression levels in P30 mice. Top left, schematic illustration of parvalbumin interneurons (in red) within the whole cortex or striatum region (yellow) in a coronal section of the mouse brain. Vertical bar graphs show cDNA level (measured by qPCR), as a measure of mRNA, in FACS-captured PV interneurons (red) from striatum (ST) and cortex (CTX), and in whole tissue preparation (yellow). Gene expression for each sample was normalized to *Actb* level. The number of animals used is indicated in the figure. * $P < 0.05$, ** $P < 0.01$, ***, non-parametric one-way ANOVA on ranks (Kruskal–Wallis test). This figure is complementary to figure 4 in the main article.

Supplementary Figure 5

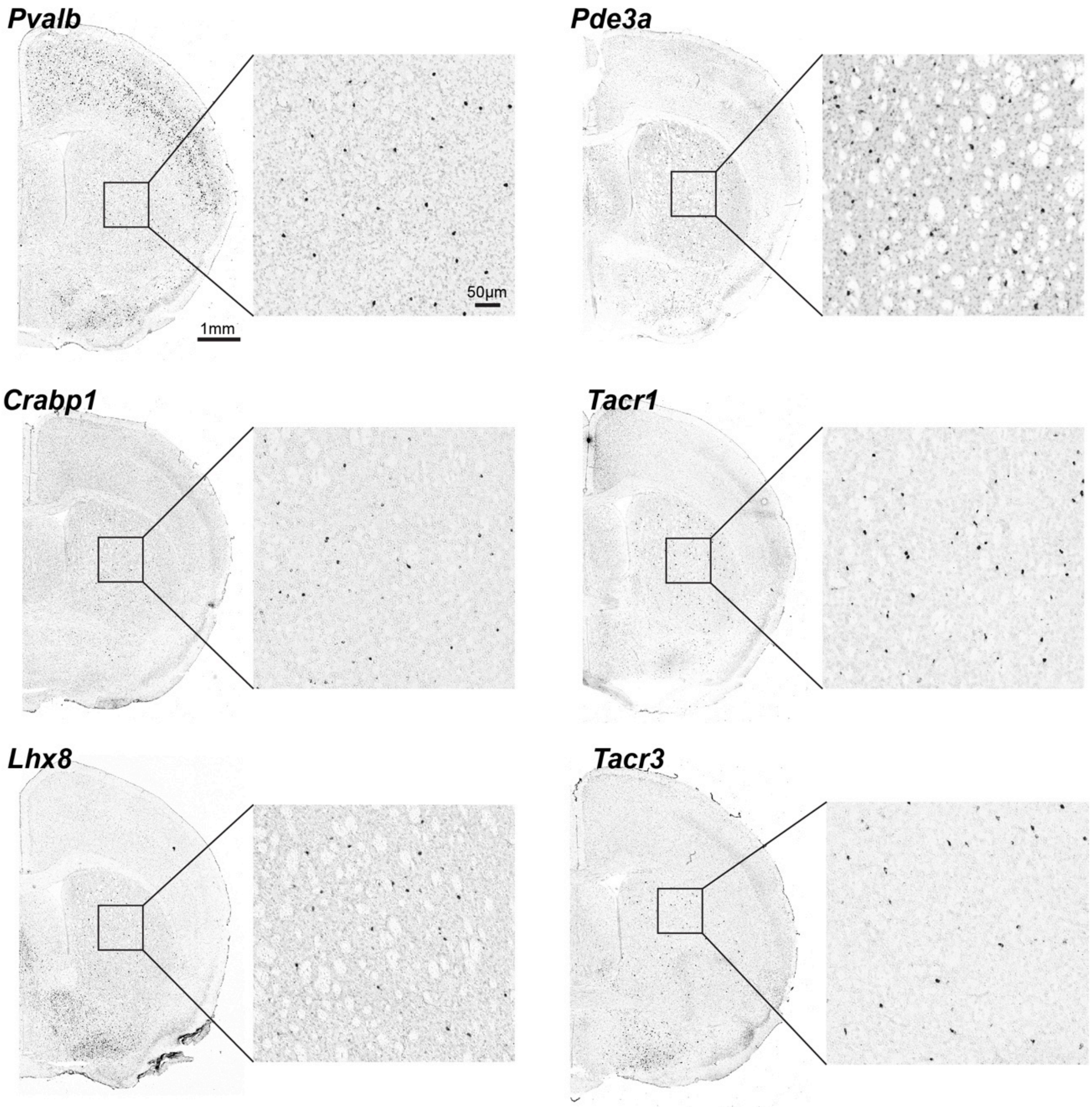

Supplementary figure 5. *In situ* expression of selected genes in the adult mouse brain. Messenger RNA expression of *Pvalb*, *Pde3a*, *Crabp1*, *Tacr1*, *Lhx8* and *Tacr3* in P56 mouse caudal brain sections detected by *in situ* hybridization and obtained from the Allen Brain Atlas (Image credit: Allen Institute). Zoomed-in pictures illustrate the similar distribution of neurons expressing the selected genes and the GDNF-expressing mouse striatal PV interneurons (published in Hidalgo-Figueroa *et al.*, 2012).

Supplementary Figure 6

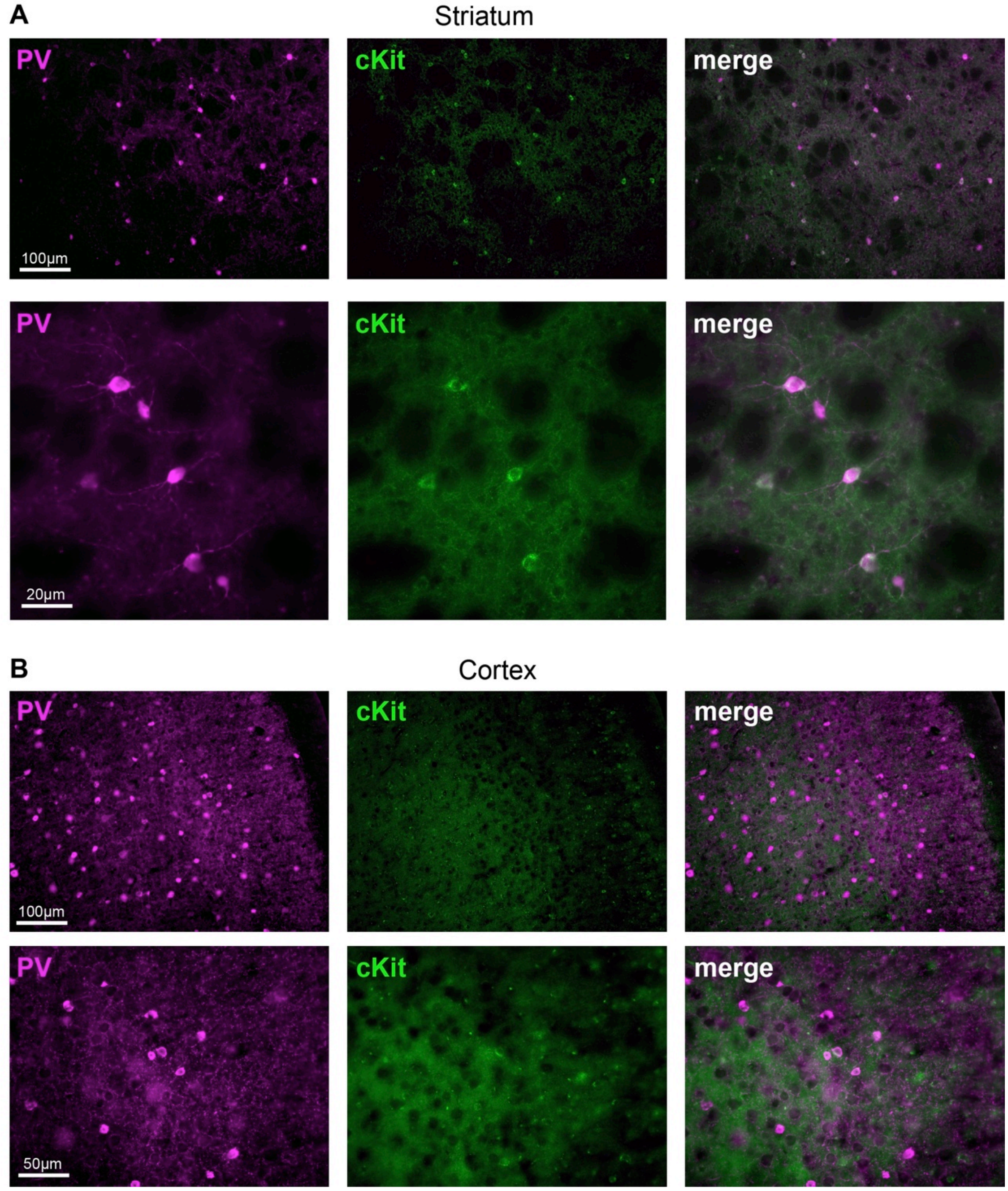

Supplementary figure 6. Immunohistochemical analysis of parvalbumin and cKit receptor in the mouse brain. Histological immunodetection of parvalbumin (PV, magenta) and cKit receptor (green) and merged photos in coronal brain sections. (**A**) Low and high magnification fluorescent microphotographs in the striatum with apparent colocalization of cKit and PV. (**B**) Low and high magnification fluorescent microphotographs in the cortex. This figure is complementary to figure 5A in the main article.

Supplementary Figure 7

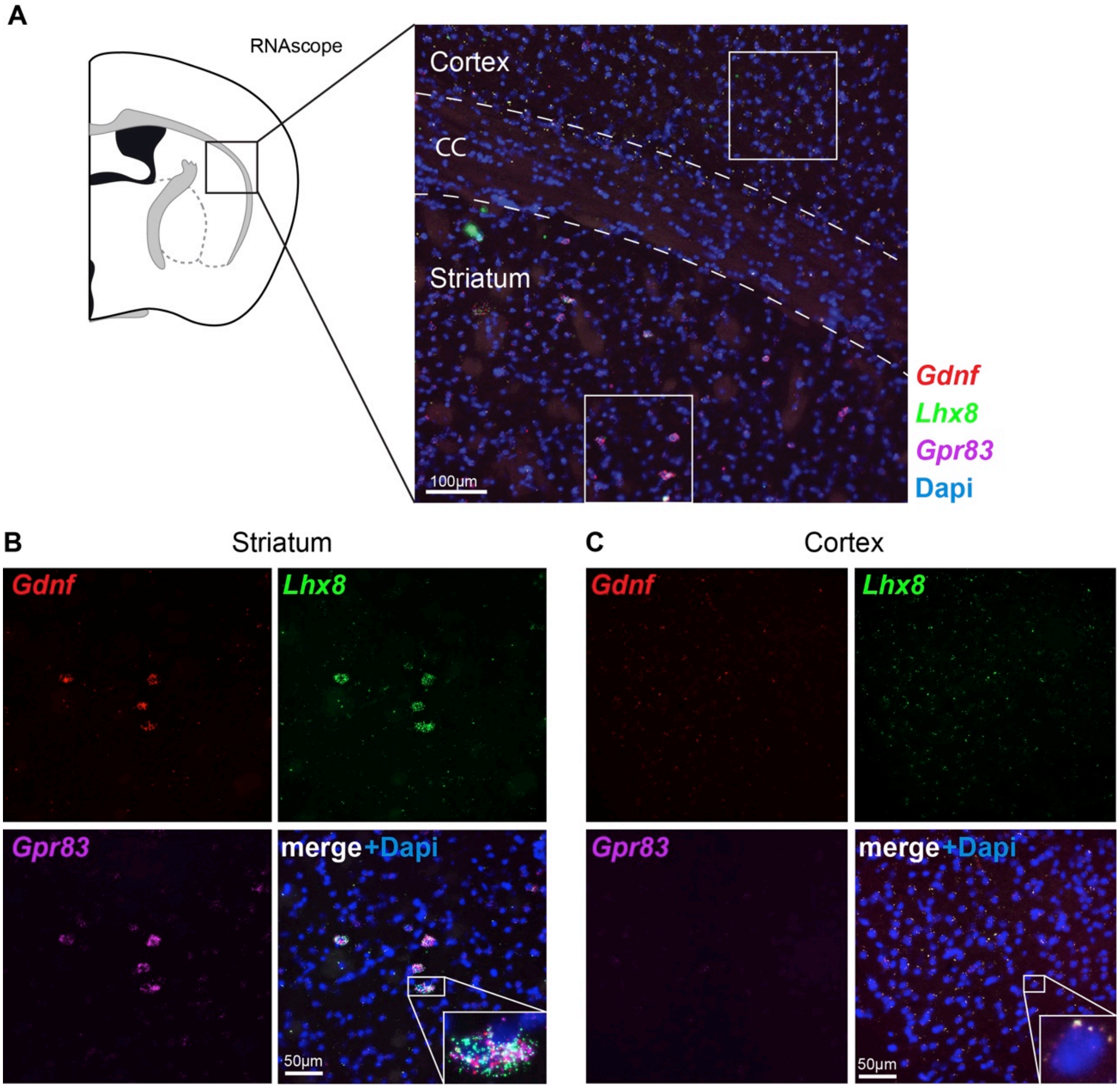

Supplementary figure 7. Expression of *Gdnf*, *Gpr83* and *Lhx8* genes in the mouse brain. (**A**) Schematic illustration of a mouse brain coronal section depicting the region of cortex (CTX) and striatum (ST) separated by the corpus callosum (CC) in the low magnification picture beside. The fluorescent microphotograph shows triple *in situ* hybridization labelling (by RNAscope method) of *Gdnf* (red), *Gpr83* (magenta) and *Lhx8* (green) genes expression across cortex and striatum, with DAPI for nuclear counterstaining (blue). (**B**) Zoomed-in region from low magnification striatum in (A) illustrates co-expression of *Gdnf*, *Gpr83* and *Lhx8*. (**C**) Zoomed-in region from low magnification picture in (A) indicates an absence of *Gdnf*, *Lhx8* and *Gpr83* in the cortex. This figure is complementary to figure 5B in the main article.

Supplementary Figure 8

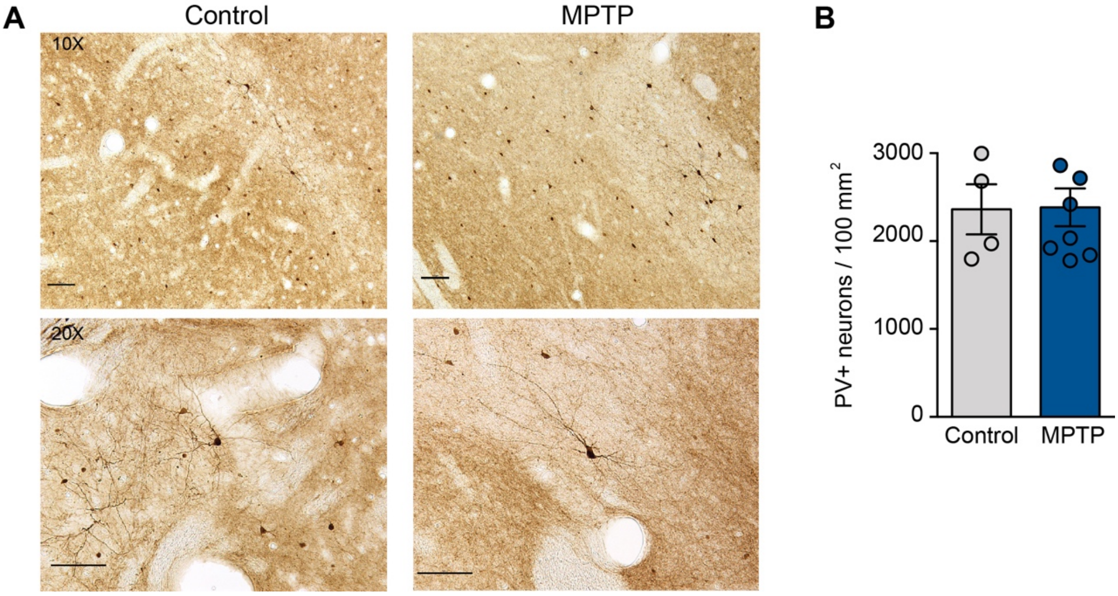

Supplementary figure 8. Parvalbumin interneurons in the caudate-putamen of normal and MPTP-treated monkey (*Macaca fascicularis*). (**A**) Representative microphotographs at 10X and 20X magnification of parvalbumin (PV) immunohistochemical staining in control (left) and MPTP-treated monkey (right). Scale bar = 100 µm. (**B**) Comparison of the number of PV neurons in the caudate-putamen region from control (N = 4) and MPTP-treated monkeys (N = 8).

Supplementary Figure 9

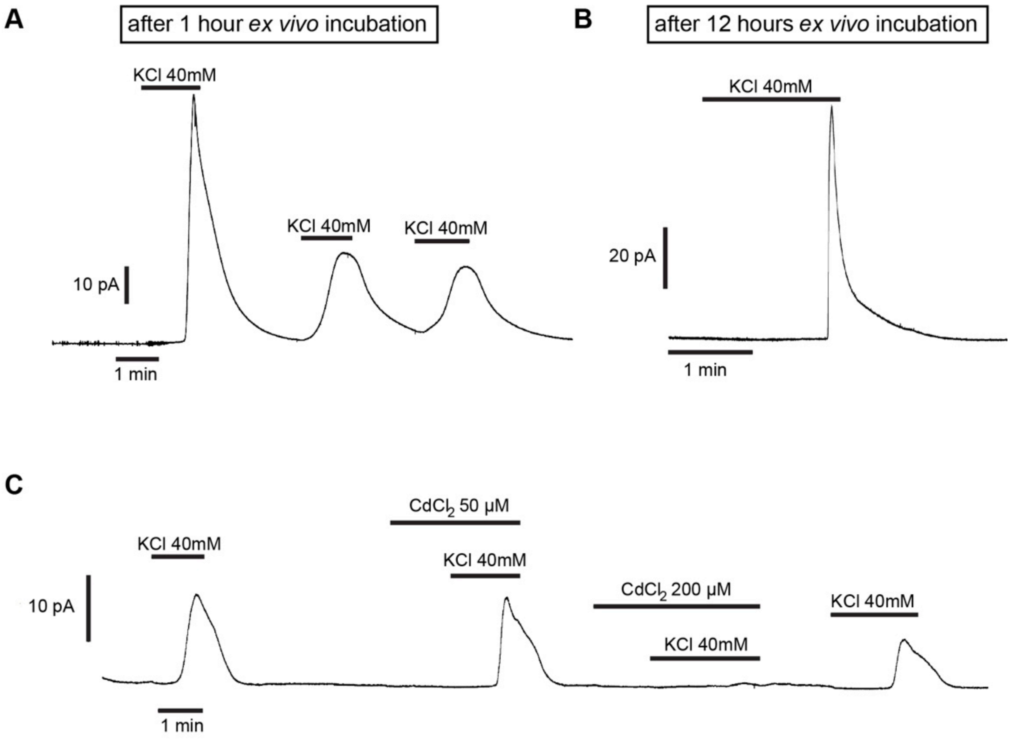

Supplementary figure 9. Viability test of *ex vivo* striatal slices by amperometric recordings. An electrically polarized amperometric carbon-fibre probe inserted in the striatum of *ex vivo* coronal brain slices was used to specifically measure catecholamine release (expressed in picoampere, pA) from dopaminergic nerve terminals. (**A** and **B**) Catecholamine release in response to applications of a high potassium (KCl 40 mM) solution to induce membrane depolarization. Experiments were performed in striatal slices that had been incubated for 1 (A) and 12 (B) hours. Note that the magnitude of dopamine release decreased in repeated stimuli due to depletion of the vesicle releasable pool. The strong signal recorded even after 12 hours incubation time indicates the good viability of the preparation. (**C**) Effect of extracellular $CdCl_2$ (a blocker of voltage-gated calcium channels) on the secretory responses to high potassium recorded in a striatal slice (1-hour incubation). Note that $CdCl_2$ at 0.2 mM produced a complete and reversible blockade of depolarization-induced catecholamine secretion. This figure is complementary to figure 8 in the main article.

Supplementary Figure 10

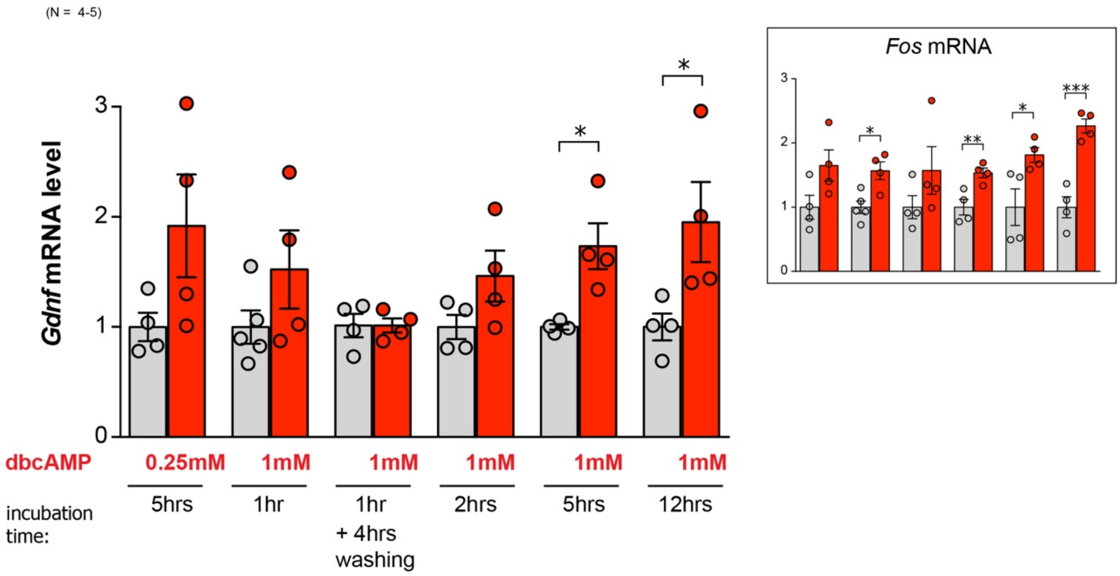

Supplementary figure 10. Effect of activation of the protein kinase A pathway on *Gdnf* gene expression in *ex vivo* conditions. Vertical bar graphs indicate *Gdnf* and *Fos* mRNA levels (measured by qPCR with *Actb* gene as internal reference) in the striatum from brain slices incubated with dibutyryl cyclic AMP (dbcAMP) at 0.25 mM or 1mM for 1, 2, 5 or 12 hours, or 1 hour followed by 4 hours without dbcAMP (washing). The level of *Fos* mRNA is indicated in the low scale bar graph. Control samples were striatum from brain slices incubated in the same conditions except that no dbcAMP was added. The number of replicates is indicated above each graph. * $P < 0.05$, ** $P < 0.01$, *** $P < 0.001$, two-tailed Student's t-test. This figure is complementary to figure 8 in the main article.

Supplementary Figure 11

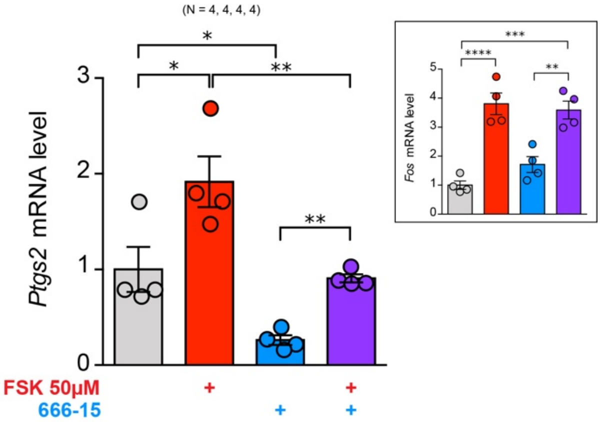

Supplementary figure 11. Effect of the CREB specific inhibitor 666-15 on prostaglandin-endoperoxide synthase 2 gene expression in *ex vivo* condition. Efficiency of 666-15 to prevent CREB pathway was tested in *ex vivo* condition. Vertical bar graphs indicate *Ptgs2* mRNA and *Fos* mRNA levels after a 5-hour incubation with FSK 50 µM and/or 10µM 666-15. * $P < 0.05$, ** $P < 0.01$, *** $P < 0.001$, **** $P < 0.0001$, one-way ANOVA with Tukey's multiple comparison test. This figure is complementary to figure 8 in the main article.

Supplementary references

Abreu CM, Prakash R, Romanienko PJ, Roig I, Keeney S, Jasin M. Shu complex SWS1-SWSAP1 promotes early steps in mouse meiotic recombination. Nat Commun 2018; 9: 3961.

Chen L, Lee JW, Chou C-L, Nair A V, Battistone MA, Păunescu TG, et al. Transcriptomes of major renal collecting duct cell types in mouse identified by single-cell RNA-seq. Proc Natl Acad Sci U S A 2017; 114: E9989–E9998.

d'Anglemont de Tassigny X, Ackroyd KJ, Chatzidaki EE, Colledge WH. Kisspeptin signaling is required for peripheral but not central stimulation of gonadotropin-releasing hormone neurons by NMDA. J Neurosci 2010; 30: 8581–8590.

Enterría-Morales D, López-López I, López-Barneo J, d'Anglemont de Tassigny X. Striatal GDNF production is independent to circulating estradiol level despite pan-neuronal activation in the female mouse. PLoS One 2016; 11

Enterría-Morales D, López-López I, López-Barneo J, d'Anglemont de Tassigny X. Role of glial cell line-derived neurotrophic factor in the maintenance of adult mesencephalic catecholaminergic neurons. Mov Disord 2020: DOI: 10.1002/mds.27986.

Hidalgo-Figueroa M, Bonilla S, Gutiérrez F, Pascual A, López-Barneo J. GDNF is predominantly expressed in the PV+ neostriatal interneuronal ensemble in normal mouse and after injury of the nigrostriatal pathway. J Neurosci 2012; 32: 864–72.

Kaiser T, Ting JT, Monteiro P, Feng G. Transgenic labeling of parvalbumin-expressing neurons with tdTomato. Neuroscience 2015; 3: 236–245.

Mejías R, Villadiego J, Pintado CO, Vime PJ, Gao L, Toledo-Aral JJ, et al. Neuroprotection by transgenic expression of glucose-6-phosphate dehydrogenase in dopaminergic nigrostriatal neurons of mice. J Neurosci 2006; 26: 4500–4508.

Paxinos G, Franklin KBJ. The mouse brain in stereotaxic coordinates. second edi. San Diego, CA: Academic Press; 2001

Urena J, Fernandez-Chacon R, Benot AR, Alvarez de Toledo GA, Lopez-Barneo J. Hypoxia induces voltage-dependent Ca2+ entry and quantal dopamine secretion in carotid body glomus cells. Proc Natl Acad Sci U S A 1994; 91: 10208–10211.

Supplementary Table 1. List of primer sequences for SYBR Green-based QPCR

Gene	5' - 3' sequence
Actb	GGCCCAGAGCAAGAGAGGTA
	CATGTCGTCCCAGTTGGTAACA
Crabp1	AGGGGGATGGCCCTAAAACT
	TGCACACCACATCATCGGC
Drd2	CCCTGGGTCGTCTATCTGGAG
	GCGTGTGTTATACAACATAGGCA
Egfr	GCCATCTGGGCCAAAGATACC
	GTCTTCGCATGAATAGGCCAAT
Flt1	CCACCTCTCTATCCGCTGG
	ACCAATGTGCTAACCGTCTTATT
Foxo1	AGTGGATGGTGAAGAGCGTG
	GAAGGGACAGATTGTGGCGA
Foxo3	GGGGAACTTCACTGGTGCTA
	GAGAGCAGATTTGGCAAAGG
Gabra2	GGACCCAGTCAGGTTGGTG
	TCCTGGTCTAAGCCGATTATCAT
Gpr12	AACGAAGACCCGAAGGTCAAT
	GGGTTCTGACTCCGCAACAG
Gpr17	ACCCGGTTGGTTTATCACTTC
	CTTGAGGGACTTGACAGGGTG
Gpr22	TCAGGAACTCGTCAGCTCTTT
	CTAGCGAGCCTCTCAGTCAGT
Gpr49	CCTACTCGAAGACTTACCCAGT
	GCATTGGGGTGAATGATAGCA
Gpr83	CATGTGTCATGTCAGTCGCTT
	TCCACTGCGATAGCTGTCAGA
Gpr88	TCCTCCACTTCGACCTCCAC
	GCCCGAGTACAGGAGAGAC
Gpr116	GGGTTTCGGTCTTGCCACA
	CTTCCTGCACCTTCTGATCCC
Grm1	TGGAACAGAGCATTGAGTTCATC
	CAATAGGCTTCTTAGTCCTGCC
Hydin	CTTGCCCCTCCGAATCAGAG
	AGGATTGCCTCGTAACAGTGA
Kcnab1	AGGACCGACTTCTGAGCAAG
	GATAGCGACAGTGCGGAATTT
Kit	GGCCTCACGAGTTCTATTTACG
	GGGGAGAGATTTCCCATCACAC
Lhx8	ACACGAGCTGCTACATTAAGGA
	CCAGTCAGTCGAGTGGATGTG
Mc3r	AAAGCCCTCACCTTGATCGG
	AGCACCATGGCGAAGAACAT
Moxd1	ACACACAGTGATCGAGTTTAGC

	CGGGATCGTCATGGTGGTA
Necab1	CCAAGGGCATGTCCATCTTCC
	TCAAGTGCGGCCAGTACATTC
Pde3a	TCCCAGTCAGGAACCAGCAT
	CAAGTTGCTTACGGCCCTC
Prokr2	CACACGCCCACCAAGTAGG
	TAGCGGGCGAGGGCAGCAATGAA
Rarres2	AGGACTGGAAAAAGCCGGAG
	ATTGGGCAGTGGACTATCCG
Rgs5	CGCACTCATGCCTGGAAAG
	TGAAGCTGGCAAATCCATAGC
Rgs9	ATGACGATCCGACACCAAGG
	CATTCTGACTCCCGTCTCTGG
Spata18	CCAAAAGCGAATCTTTACAAGCA
	TGTTCGATGAGTTCGATGCAAT
Sst	ACCGGGAAACAGGAACTGG
	TTGCTGGGTTCGAGTTGGC
Tacr1	GCTGCTCTCTTCGCCAGTAT
	GCCAGGACCCAGATGACAAA
Tacr3	GTTCACAGCGAGTGGTACTTT
	TCCGATGACAATCTTAGTGGCT
Tmem212	GGTACACAGGATGGAGCGTTT
	GCTTCCCACAAGTGTCTCTGG

Supplementary Table 2. Differentially expressed (DE) genes between striatum and cortex (ST/CTX) PV interneurons from *PV-CRE; tdTomato* mice sorted by logFC (log2 fold change). FDR (false discovery rate).

Gene	**Gene Name**	**logFC**	***P* Value**	**FDR**
Tmem212	transmembrane protein 212	5.191818057	3.0856E-13	7.62977E-09
Fam183b	family with sequence similarity 183, member B	4.439783468	1.4812E-10	2.03476E-07
Rsph4a	radial spoke head 4 homolog A (Chlamydomonas)	4.08932254	5.26327E-12	4.15703E-08
Mia	melanoma inhibitory activity	4.088307579	3.71895E-10	3.53686E-07
Tm4sf1	transmembrane 4 superfamily member 1	3.656843644	1.09293E-11	4.15703E-08
Gpr83	G protein-coupled receptor 83	3.529996187	0.000282427	0.01467139
Necab1	N-terminal EF-hand calcium binding protein 1	3.425496437	3.18602E-06	0.000421287
Fam216b	family with sequence similarity 216, member B	3.331914874	2.70578E-11	6.90401E-08
Egfr	epidermal growth factor receptor	3.290963401	3.6293E-07	7.14385E-05
Il1rapl2	interleukin 1 receptor accessory protein-like 2	3.265066344	2.61996E-05	0.002281117
Sntn	sentan, cilia apical structure protein	3.224261842	8.98152E-11	1.38804E-07
Spata18	spermatogenesis associated 18	3.206739106	2.548E-11	6.90401E-08
Lgi1	leucine-rich repeat LGI family, member 1	3.142808041	9.06385E-06	0.000978698
Capsl	calcyphosine-like	3.139851085	3.18836E-10	3.28494E-07
Cd24a	CD24a antigen	3.070187919	8.40333E-08	2.18725E-05
Crabp1	cellular retinoic acid binding protein I	2.972734712	9.94458E-07	0.000166148
Rarres2	retinoic acid receptor responder (tazarotene induced) 2	2.970709167	1.01063E-10	1.47E-07
Nme5	NME/NM23 family member 5	2.916447969	1.28403E-08	4.88465E-06
Pifo	primary cilia formation	2.88796238	6.53166E-10	5.56925E-07
Hapln1	hyaluronan and proteoglycan link protein 1	2.884278156	3.53658E-06	0.000460257
Ccdc153	coiled-coil domain containing 153	2.820190928	3.01254E-10	3.23874E-07
Ctla2a	cytotoxic T lymphocyte-associated protein 2 alpha	2.817245398	6.55078E-05	0.004788444
Pcp4	Purkinje cell protein 4	2.784693599	9.61994E-06	0.001016549
Ly6c2	lymphocyte antigen 6 complex, locus C2	2.776240192	9.97332E-05	0.006629308
Dgkb	diacylglycerol kinase, beta	2.773397177	4.45426E-10	4.07928E-07
Galnt14	UDP-N-acetyl-alpha-D-galactosamine:polypeptide N-acetylgalactosaminyltransferase 14	2.748700866	3.25373E-05	0.002718076

Moxd1	monooxygenase, DBH-like 1	2.700002663	1.08127E-05	0.001118681
Rgs22	regulator of G-protein signalling 22	2.686194441	1.81361E-10	2.36027E-07
Enkur	enkurin, TRPC channel interacting protein	2.660678336	2.46534E-10	2.90288E-07
Cfap54	cilia and flagella associated protein 54	2.656423922	8.71964E-11	1.38804E-07
Efcab10	EF-hand calcium binding domain 10	2.576755818	2.56437E-07	5.37366E-05
Cfap206	cilia and flagella associated protein 206	2.54252278	1.75758E-09	1.15859E-06
Cnr1	cannabinoid receptor 1 (brain)	2.507297232	2.66152E-05	0.002309168
Nrcam	neuronal cell adhesion molecule	2.494402037	9.23587E-06	0.000988638
Csrp2	cysteine and glycine-rich protein 2	2.396654959	1.06712E-08	4.25593E-06
Lbp	lipopolysaccharide binding protein	2.395564525	1.07008E-11	4.15703E-08
Pthlh	parathyroid hormone-like peptide	2.385286057	0.000103222	0.006824519
Ppil6	peptidylprolyl isomerase (cyclophilin)-like 6	2.364861496	2.84365E-08	8.78937E-06
Efcab1	EF hand calcium binding domain 1	2.358064337	2.79209E-11	6.90401E-08
Rab3c	RAB3C, member RAS oncogene family	2.340810984	0.000819732	0.030450399
Adgrl4	adhesion G protein-coupled receptor L4	2.323812612	5.17962E-05	0.00395968
Kcnab1	potassium voltage-gated channel, shaker-related subfamily, beta member 1	2.301044474	0.000177097	0.010401612
Chml	choroideremia-like	2.286680723	0.000124673	0.007884397
Mc4r	melanocortin 4 receptor	2.28374035	9.91661E-05	0.006609381
Lamb1	laminin B1	2.277310175	2.44572E-05	0.002159829
Lrrc74b	leucine rich repeat containing 74B	2.258460456	3.66584E-10	3.53686E-07
Gm10400	predicted gene 10400	2.226190626	1.67374E-05	0.001567669
Morn5	MORN repeat containing 5	2.224370095	2.77842E-08	8.69646E-06
Gsta4	glutathione S-transferase, alpha 4	2.187143635	6.39327E-09	2.81597E-06
Wdr63	WD repeat domain 63	2.173925439	1.51071E-09	1.03765E-06
Kit	kit oncogene	2.159781356	7.3301E-06	0.00082387
Dnah12	dynein, axonemal, heavy chain 12	2.149130614	1.48152E-08	5.4677E-06
Stoml3	stomatin (Epb7.2)-like 3	2.100597331	5.93184E-09	2.71623E-06
Gpr88	G-protein coupled receptor 88	2.098494197	9.21616E-07	0.000156088
Vim	vimentin	2.086091742	9.41418E-08	2.37535E-05

Dnah6	dynein, axonemal, heavy chain 6	2.08013377	3.62088E-11	8.13941E-08
Kcna4	potassium voltage-gated channel, shaker-related subfamily, member 4	2.072408716	3.58643E-06	0.000461884
Adamts5	a disintegrin-like and metallopeptidase (reprolysin type) with thrombospondin type 1 motif, 5 (aggrecanase-2)	2.069978371	8.74485E-06	0.000956787
Pltp	phospholipid transfer protein	2.065309918	2.58992E-12	3.20204E-08
Zbbx	zinc finger, B-box domain containing	2.057498625	2.4178E-09	1.4554E-06
Cdh8	cadherin 8	2.054388544	0.000767475	0.02954606
Grip1	glutamate receptor interacting protein 1	2.04586029	0.000858842	0.031461619
Slc4a4	solute carrier family 4 (anion exchanger), member 4	2.018226026	2.96507E-05	0.002502293
Adgrf5	adhesion G protein-coupled receptor F5	2.015945947	0.000199937	0.011551032
Cdhr3	cadherin-related family member 3	2.014279209	3.94724E-09	1.99191E-06
LOC101056100	centrin-4 pseudogene	2.012483487	6.53279E-06	0.000740992
Rsph1	radial spoke head 1 homolog (Chlamydomonas)	2.00687824	6.70034E-08	1.7815E-05
Igfbp7	insulin-like growth factor binding protein 7	1.983414211	0.000322142	0.01606329
Ppp1r36	protein phosphatase 1, regulatory subunit 36	1.973735497	6.49129E-09	2.81597E-06
Ctla2b	cytotoxic T lymphocyte-associated protein 2 beta	1.965390209	0.001447482	0.044964682
Rit2	Ras-like without CAAX 2	1.959778213	0.001584109	0.047193099
Nxph1	neurexophilin 1	1.940352449	0.000265474	0.01396674
Pygm	muscle glycogen phosphorylase	1.927079123	0.000232418	0.012714622
Resp18	regulated endocrine-specific protein 18	1.924199242	0.000937904	0.033659732
Dthd1	death domain containing 1	1.918473087	5.42997E-11	9.59048E-08
Fstl5	follistatin-like 5	1.916888438	0.001260649	0.040961978
Gabra2	gamma-aminobutyric acid (GABA) A receptor, subunit alpha 2	1.909039642	0.000161242	0.009653846
Opn3	opsin 3	1.897063766	1.17972E-05	0.001185807
Pde3a	phosphodiesterase 3A, cGMP inhibited	1.886900044	2.85586E-05	0.002443493
Dynlrb2	dynein light chain roadblock-type 2	1.886366274	3.09615E-07	6.32714E-05
Prelp	proline arginine-rich end leucine-rich repeat	1.884509749	3.23132E-09	1.77558E-06
Map3k19	mitogen-activated protein kinase kinase kinase 19	1.873181237	1.10483E-09	8.27849E-07
Rgs5	regulator of G-protein signaling 5	1.852911427	0.000136374	0.00847268

Ndst4	N-deacetylase/N-sulfotransferase (heparin glucosaminyl) 4	1.837773169	2.82529E-05	0.002425729
Spef2	sperm flagellar 2	1.823500535	2.4606E-09	1.4554E-06
Iqca	IQ motif containing with AAA domain	1.810059129	1.17682E-11	4.15703E-08
Gm7173	predicted gene 7173	1.752927923	3.0249E-07	6.23306E-05
Mir3967	microRNA 3967	1.752862175	0.001398514	0.043915102
Astn2	astrotactin 2	1.751026318	3.89847E-06	0.000481988
Mlf1	myeloid leukemia factor 1	1.745608476	2.16093E-08	7.04102E-06
Gpc3	glypican 3	1.74395844	0.000215096	0.01214309
Ly6c1	lymphocyte antigen 6 complex, locus C1	1.735311128	0.000145481	0.00894854
Hydin	HYDIN, axonemal central pair apparatus protein	1.733398994	8.13782E-12	4.15703E-08
Got1l1	glutamic-oxaloacetic transaminase 1-like 1	1.732807238	1.00208E-07	2.45332E-05
Daw1	dynein assembly factor with WDR repeat domains 1	1.728246764	4.47016E-08	1.25606E-05
Pla2g7	phospholipase A2, group VII (platelet-activating factor acetylhydrolase, plasma)	1.726454326	0.000352715	0.017067695
Acta2	actin, alpha 2, smooth muscle, aorta	1.717267574	1.19617E-06	0.000190824
Dpp10	dipeptidylpeptidase 10	1.70916946	0.000537464	0.023051368
Ccdc108	coiled-coil domain containing 108	1.704074001	4.72119E-11	8.98008E-08
Prokr2	prokineticin receptor 2	1.696183754	8.9005E-05	0.00601319
Lrrc34	leucine rich repeat containing 34	1.695302496	1.02379E-05	0.001068149
Gm5454	predicted gene 5454	1.686795004	7.50258E-05	0.005300467
Bbox1	butyrobetaine (gamma), 2-oxoglutarate dioxygenase 1 (gamma-butyrobetaine hydroxylase)	1.682099452	2.05741E-06	0.000294068
Lrrc6	leucine rich repeat containing 6 (testis)	1.680484821	2.24417E-06	0.000312251
Cfap44	cilia and flagella associated protein 44	1.669172534	1.88636E-08	6.47835E-06
Gstm1	glutathione S-transferase, mu 1	1.66848144	0.000250306	0.013339025
Chl1	cell adhesion molecule L1-like	1.661800895	0.000877251	0.031946668
Cox8b	cytochrome c oxidase subunit VIIIb	1.661724923	1.31007E-05	0.00129576
Rgs9	regulator of G-protein signaling 9	1.65181711	4.91658E-07	9.28033E-05
Crygn	crystallin, gamma N	1.647346131	4.86169E-08	1.33572E-05
Dlx6os1	distal-less homeobox 6, opposite strand 1	1.637754747	0.00149094	0.045853831

Spa17	sperm autoantigenic protein 17	1.635137065	1.14258E-08	4.41448E-06
Anxa5	annexin A5	1.634013133	2.84266E-06	0.000382163
Wdr49	WD repeat domain 49	1.62657745	3.41675E-09	1.83665E-06
Ccdc113	coiled-coil domain containing 113	1.620992891	9.34472E-09	3.78798E-06
Igfbp4	insulin-like growth factor binding protein 4	1.5914319	6.28071E-05	0.004622115
Vwa3a	von Willebrand factor A domain containing 3A	1.589874345	4.00955E-11	8.26201E-08
Spag17	sperm associated antigen 17	1.579446659	7.72243E-10	6.36508E-07
Lrrc23	leucine rich repeat containing 23	1.578203361	1.09242E-08	4.28768E-06
Apold1	apolipoprotein L domain containing 1	1.574154504	0.000123141	0.007827513
Lgr5	leucine rich repeat containing G protein coupled receptor 5	1.567810909	9.47304E-05	0.006347963
Tmem47	transmembrane protein 47	1.567422144	7.22103E-05	0.00511617
Ly6a	lymphocyte antigen 6 complex, locus A	1.563969824	0.000308668	0.015640247
Necab2	N-terminal EF-hand calcium binding protein 2	1.557972127	3.59206E-05	0.002960699
Frmpd4	FERM and PDZ domain containing 4	1.557288206	0.000744213	0.029123958
Akap14	A kinase (PRKA) anchor protein 14	1.550505542	7.20622E-09	3.02014E-06
Iqcg	IQ motif containing G	1.549272169	1.98686E-07	4.30958E-05
Anxa2	annexin A2	1.545210183	6.5254E-07	0.000117776
Pde1b	phosphodiesterase 1B, Ca2+-calmodulin dependent	1.542758373	0.000968463	0.034259216
Cdhr4	cadherin-related family member 4	1.537641518	8.55521E-10	6.82402E-07
Cd55	CD55 molecule, decay accelerating factor for complement	1.535640893	6.47323E-09	2.81597E-06
Cfap61	cilia and flagella associated protein 61	1.535066796	1.78632E-09	1.15859E-06
Clu	clusterin	1.521272687	5.29569E-09	2.5182E-06
Mdh1b	malate dehydrogenase 1B, NAD (soluble)	1.520158054	1.12599E-07	2.70314E-05
Ifitm3	interferon induced transmembrane protein 3	1.501572617	1.44267E-05	0.001398939
Gria4	glutamate receptor, ionotropic, AMPA4 (alpha 4)	1.488011821	0.000228923	0.012579075
Fn1	fibronectin 1	1.482894463	0.000111057	0.00726486
Maats1	MYCBP-associated, testis expressed 1	1.470834032	7.48349E-09	3.08407E-06
Dnah3	dynein, axonemal, heavy chain 3	1.467280566	3.54851E-09	1.86689E-06
Cd93	CD93 antigen	1.464288341	0.001360707	0.043025819

Fxyd1	FXYD domain-containing ion transport regulator 1	1.460576778	1.01627E-07	2.46367E-05
Dpp6	dipeptidylpeptidase 6	1.460442308	0.000323514	0.01606329
Lrrc51	leucine rich repeat containing 51	1.458409789	1.19914E-07	2.82391E-05
Mak	male germ cell-associated kinase	1.457951917	3.24539E-07	6.52428E-05
Dnah9	dynein, axonemal, heavy chain 9	1.455593843	1.37916E-09	1.00153E-06
Kcnmb1	potassium large conductance calcium-activated channel, subfamily M, beta member 1	1.453687458	3.11281E-09	1.74933E-06
Gm11992	predicted gene 11992	1.453462815	8.63589E-08	2.22437E-05
Pou3f2	POU domain, class 3, transcription factor 2	1.445552944	0.000241124	0.013018069
Cfap161	cilia and flagella associated protein 161	1.445228277	8.89816E-10	6.87577E-07
Tekt1	tektin 1	1.4381516	7.81316E-08	2.05528E-05
Lrriq1	leucine-rich repeats and IQ motif containing 1	1.436134745	1.42409E-08	5.33537E-06
Tmem255a	transmembrane protein 255A	1.430489733	9.55078E-06	0.001013571
Ddah1	dimethylarginine dimethylaminohydrolase 1	1.429028326	0.001141738	0.038099547
Vtn	vitronectin	1.425241607	0.000818903	0.030450399
Dnah11	dynein, axonemal, heavy chain 11	1.422512697	3.78217E-09	1.94837E-06
Cyr61	cysteine rich protein 61	1.403245736	3.34469E-05	0.002773006
Spag6l	sperm associated antigen 6-like	1.402865149	3.97166E-08	1.14194E-05
Efhb	EF hand domain family, member B	1.40170307	3.07475E-08	9.16015E-06
Penk	preproenkephalin	1.398417599	0.000481715	0.021346515
Drc1	dynein regulatory complex subunit 1	1.385266284	9.69338E-08	2.39688E-05
Lrrc48	leucine rich repeat containing 48	1.382312602	4.29522E-09	2.12416E-06
Syt10	synaptotagmin X	1.381602655	2.30641E-05	0.002051463
Gpx8	glutathione peroxidase 8 (putative)	1.376854319	2.50821E-05	0.002207135
Pcbd1	pterin 4 alpha carbinolamine dehydratase/dimerization cofactor of hepatocyte nuclear factor 1 alpha (TCF1) 1	1.376467841	0.00089864	0.032486377
Lrrc9	leucine rich repeat containing 9	1.375025999	5.549E-08	1.49141E-05
Adam23	a disintegrin and metallopeptidase domain 23	1.369032041	2.67654E-05	0.002314084
Drd2	dopamine receptor D2	1.364573597	0.000174111	0.010299617
Ccdc146	coiled-coil domain containing 146	1.35626796	7.31868E-07	0.000130193

Slc25a18	solute carrier family 25 (mitochondrial carrier), member 18	1.355666792	0.001504953	0.046075873
Ppm1l	protein phosphatase 1 (formerly 2C)-like	1.352893694	0.00031965	0.015999992
Pcdh15	protocadherin 15	1.351527276	0.000471689	0.021089554
Slc35f1	solute carrier family 35, member F1	1.349691385	3.73644E-05	0.003059305
Flt1	FMS-like tyrosine kinase 1	1.34426277	0.000335488	0.016504014
Fbxl13	F-box and leucine-rich repeat protein 13	1.340171381	2.0073E-08	6.79924E-06
Slco1a4	solute carrier organic anion transporter family, member 1a4	1.335638484	0.000336955	0.016504014
Emcn	endomucin	1.327770674	0.00166103	0.048548793
Cacnb2	calcium channel, voltage-dependent, beta 2 subunit	1.32471847	0.000766337	0.02954606
Spag16	sperm associated antigen 16	1.321187617	1.41762E-09	1.00153E-06
Alcam	activated leukocyte cell adhesion molecule	1.309715819	0.000779784	0.029844552
Skp2	S-phase kinase-associated protein 2 (p45)	1.305900617	9.11207E-05	0.006122669
Pdlim3	PDZ and LIM domain 3	1.305279197	0.001399486	0.043915102
Map3k7cl	Map3k7 C-terminal like	1.302044161	1.62744E-05	0.001530102
Cxcr4	chemokine (C-X-C motif) receptor 4	1.289694715	0.000235056	0.012830505
Cfap43	cilia and flagella associated protein 43	1.281690002	2.69916E-07	5.60859E-05
Cetn4	centrin 4	1.279392872	2.67025E-06	0.000364792
Iqub	IQ motif and ubiquitin domain containing	1.277830859	2.51869E-05	0.002208502
Dnaic1	dynein, axonemal, intermediate chain 1	1.277757973	1.62126E-08	5.89543E-06
Mlc1	megalencephalic leukoencephalopathy with subcortical cysts 1 homolog (human)	1.276142495	0.000805148	0.030079684
Saxo2	stablizer of axonemal microtubules 2	1.274011731	1.82165E-08	6.34421E-06
Cdc42ep3	CDC42 effector protein (Rho GTPase binding) 3	1.270249017	0.000753657	0.029283774
Tmem196	transmembrane protein 196	1.265553489	0.001545835	0.046329675
Cdkl4	cyclin-dependent kinase-like 4	1.263543526	1.81402E-05	0.001686288
Acot5	acyl-CoA thioesterase 5	1.249696135	3.25537E-06	0.000425902
Tmem232	transmembrane protein 232	1.248083326	2.93763E-08	8.92091E-06
Lrrtm3	leucine rich repeat transmembrane neuronal 3	1.244275714	0.001724562	0.049789517
Nek5	NIMA (never in mitosis gene a)-related expressed kinase 5	1.242928746	1.33306E-07	3.0806E-05
Gna14	guanine nucleotide binding protein, alpha 14	1.23795346	5.89871E-05	0.004406567

Ak7	adenylate kinase 7	1.234195263	7.75168E-07	0.000133766
Emp2	epithelial membrane protein 2	1.233389769	6.27157E-06	0.000714641
Myl9	myosin, light polypeptide 9, regulatory	1.231472752	6.38076E-05	0.004681811
Gcnt2	glucosaminyl (N-acetyl) transferase 2, I-branching enzyme	1.225263474	0.000214022	0.012110105
Ptprg	protein tyrosine phosphatase, receptor type, G	1.224012913	8.4544E-06	0.000933267
Dmkn	dermokine	1.211168788	3.39354E-08	9.98953E-06
Odf3b	outer dense fiber of sperm tails 3B	1.205308371	2.00306E-10	2.47648E-07
Kcnd2	potassium voltage-gated channel, Shal-related family, member 2	1.201506877	0.000682305	0.02725584
Plk2	polo-like kinase 2	1.192965865	0.000376958	0.017822241
Rbp1	retinol binding protein 1, cellular	1.192241224	4.50132E-07	8.62824E-05
Ppp1r32	protein phosphatase 1, regulatory subunit 32	1.179528262	1.82736E-09	1.15859E-06
Sgcz	sarcoglycan zeta	1.173554864	1.4289E-05	0.001391043
Riiad1	regulatory subunit of type II PKA R-subunit (RIIa) domain containing 1	1.172883398	2.4767E-09	1.4554E-06
Megf11	multiple EGF-like-domains 11	1.169780486	5.65886E-05	0.004253092
Fat4	FAT atypical cadherin 4	1.159517322	1.94958E-05	0.001785455
Rapgef5	Rap guanine nucleotide exchange factor (GEF) 5	1.150433966	0.001019723	0.035166935
Kcnd3	potassium voltage-gated channel, Shal-related family, member 3	1.147247867	4.41336E-05	0.003453456
Cfap46	cilia and flagella associated protein 46	1.143456098	5.77482E-06	0.000667261
Adgb	androglobin	1.139064481	1.61933E-05	0.001528292
Hs3st2	heparan sulfate (glucosamine) 3-O-sulfotransferase 2	1.137949465	7.70759E-05	0.005398206
Sox9	SRY (sex determining region Y)-box 9	1.131324841	2.10706E-06	0.000299433
Cdh13	cadherin 13	1.131308292	0.000469642	0.021089554
Ccdc96	coiled-coil domain containing 96	1.131059094	0.000112671	0.007350962
Wdr78	WD repeat domain 78	1.129675965	6.64226E-07	0.000119017
Nwd2	NACHT and WD repeat domain containing 2	1.129666543	0.001508462	0.046075873
Ndrg2	N-myc downstream regulated gene 2	1.113979599	0.000349818	0.016993998
Rsph9	radial spoke head 9 homolog (Chlamydomonas)	1.113938588	1.45475E-05	0.00140514
Ndn	necdin	1.109118086	0.001010368	0.035166935
Pld5	phospholipase D family, member 5	1.107043106	0.000669457	0.026829265

Bcl11b	B cell leukemia/lymphoma 11B	1.104929885	0.001067558	0.03621285
Pygo1	pygopus 1	1.103948982	0.000702755	0.027847777
Nfib	nuclear factor I/B	1.09961106	1.53684E-05	0.00146724
Cep126	centrosomal protein 126	1.096071309	0.000169573	0.010128101
Gm973	predicted gene 973	1.096068959	1.83321E-07	4.05687E-05
Armc3	armadillo repeat containing 3	1.095676828	2.2629E-06	0.000312596
Plp2	proteolipid protein 2	1.094159809	1.12508E-06	0.000181828
Klk6	kallikrein related-peptidase 6	1.089232001	0.000226162	0.012482838
Cd59a	CD59a antigen	1.085317779	0.000952791	0.033850086
Plpp1	phospholipid phosphatase 1	1.072218432	0.000662529	0.026690949
Dcx	doublecortin	1.067026208	0.000754388	0.029283774
Htra4	HtrA serine peptidase 4	1.064723003	0.000374087	0.017754394
Gm10714	predicted gene 10714	1.063072714	2.05775E-08	6.87593E-06
Ccnd2	cyclin D2	1.062656445	0.00031651	0.0159072
Ccdc81	coiled-coil domain containing 81	1.057908099	1.03084E-06	0.000169988
Mro	maestro	1.05724834	3.97776E-06	0.000489344
Gm867	predicted gene 867	1.051532189	3.70085E-06	0.000471705
Nnat	neuronatin	1.05114586	1.49609E-05	0.001433866
Dnajb13	DnaJ heat shock protein family (Hsp40) member B13	1.048980211	2.53093E-09	1.4554E-06
Slc6a20a	solute carrier family 6 (neurotransmitter transporter), member 20A	1.037891889	0.001713125	0.049602403
Nid1	nidogen 1	1.035691537	0.000290347	0.014957082
Fam166b	family with sequence similarity 166, member B	1.03094977	6.83289E-09	2.91305E-06
Dusp18	dual specificity phosphatase 18	1.02822782	0.000317624	0.015930818
Cfap52	cilia and flagella associated protein 52	1.027805991	1.68041E-07	3.77741E-05
Lxn	latexin	1.027160874	0.00026247	0.013838153
Erich2	glutamate rich 2	1.025225625	3.94536E-05	0.003198591
Bmp6	bone morphogenetic protein 6	1.023800722	5.53109E-06	0.000654389
Cfap77	cilia and flagella associated protein 77	1.022798204	1.39965E-06	0.000216308
Pde10a	phosphodiesterase 10A	1.022149254	0.000119328	0.007697094

Dnali1	dynein, axonemal, light intermediate polypeptide 1	1.02130444	7.61397E-07	0.000133766
Nexn	nexilin	1.019167731	4.88498E-06	0.000586363
Lrguk	leucine-rich repeats and guanylate kinase domain containing	1.018073819	9.56492E-07	0.000160892
Cd55b	CD55 molecule, decay accelerating factor for complement B	1.016400578	3.75451E-07	7.25296E-05
Dpy19l2	dpy-19-like 2 (C. elegans)	1.015674107	1.60768E-06	0.000242396
Prrg4	proline rich Gla (G-carboxyglutamic acid) 4 (transmembrane)	1.012037952	2.95836E-08	8.92091E-06
Sh3bgrl	SH3-binding domain glutamic acid-rich protein like	1.003634981	0.00147767	0.045547146
Epha4	Eph receptor A4	1.00106891	0.001526221	0.046088946
Tmem163	transmembrane protein 163	-1.061806007	0.000738473	0.029123159
Kndc1	kinase non-catalytic C-lobe domain (KIND) containing 1	-1.064129918	0.000482985	0.021364512
Nfasc	neurofascin	-1.066966183	0.000237867	0.012927874
Tmem2	transmembrane protein 2	-1.08756272	1.49439E-05	0.001433866
Gm11549	predicted gene 11549	-1.101544722	8.71071E-05	0.00592127
Rras2	related RAS viral (r-ras) oncogene 2	-1.122431731	8.0483E-06	0.000896443
Parvb	parvin, beta	-1.190778308	0.000984897	0.034593112
Tcf7l2	transcription factor 7 like 2, T cell specific, HMG box	-1.200573736	0.001544882	0.046329675
Tssc4	tumor-suppressing subchromosomal transferable fragment 4	-1.212064678	6.64677E-05	0.004833964
Prom1	prominin 1	-1.216908854	0.000221564	0.012315813
C130030K03Rik	proteasome (prosome, macropain) subunit, alpha type 6 pseudogene	-1.246019685	6.05035E-05	0.004479251
Frmd4a	FERM domain containing 4A	-1.310687542	0.000564556	0.023985871
Cnksr3	Cnksr family member 3	-1.417830761	0.000106087	0.006976645
9630013A20Rik	RIKEN cDNA 9630013A20 gene	-1.729464938	2.26685E-05	0.002030884

Nrn1	neuritin 1	-1.868739515	5.61413E-05	0.004245275

Supplementary Table 3. Differentially expressed (DE) genes between striatum and cortex (ST/CTX) PV interneurons from *PV-tdTomato* mice sorted by logFC (log2 fold change). FDR (false discovery rate).

Gene	**Gene Name**	**logFC**	***P* Value**	**FDR**
Gpr83	G protein-coupled receptor 83	3.768634171	0.000151697	0.011613024
Trh	thyrotropin releasing hormone	3.578675002	1.39112E-08	1.18615E-05
Tmem212	transmembrane protein 212	3.534484552	8.00431E-11	6.59742E-07
Crabp1	cellular retinoic acid binding protein I	3.502584566	1.25701E-07	5.55038E-05
Il1rapl2	interleukin 1 receptor accessory protein-like 2	3.32962109	2.11814E-05	0.002436058
Rsph4a	radial spoke head 4 homolog A (Chlamydomonas)	3.252006399	1.40157E-10	7.10194E-07
Tm4sf1	transmembrane 4 superfamily member 1	2.963971139	2.19032E-10	7.10194E-07
Tacr3	tachykinin receptor 3	2.911769265	1.95414E-08	1.42118E-05
Th	tyrosine hydroxylase	2.842279537	2.40757E-06	0.000437736
Spata18	spermatogenesis associated 18	2.789784705	1.8517E-10	7.10194E-07
Fam183b	family with sequence similarity 183, member B	2.751703498	1.01331E-07	4.64003E-05
Ccdc153	coiled-coil domain containing 153	2.678206031	6.21779E-10	1.18267E-06
Lhx8	LIM homeobox protein 8	2.61786205	4.52108E-08	2.66173E-05
Capsl	calcyphosine-like	2.525839803	6.49137E-09	7.41057E-06
Fam216b	family with sequence similarity 216, member B	2.469184788	1.84895E-09	2.85743E-06
Rsph1	radial spoke head 1 homolog (Chlamydomonas)	2.293620995	1.13421E-08	1.07739E-05
Moxd1	monooxygenase, DBH-like 1	2.245560253	7.80335E-05	0.006746626
Gpc3	glypican 3	2.221204776	1.79743E-05	0.002211202
Mc4r	melanocortin 4 receptor	2.183818315	0.000154141	0.011702746
Rarres2	retinoic acid receptor responder (tazarotene induced) 2	2.180510054	7.47289E-09	7.71718E-06
Pifo	primary cilia formation	2.105873856	4.80165E-08	2.76117E-05
Cfap206	cilia and flagella associated protein 206	2.083544502	2.62714E-08	1.64059E-05
Tacr1	tachykinin receptor 1	2.039512344	7.65646E-05	0.006700962
Mc3r	melanocortin 3 receptor	2.02599104	3.70341E-07	0.000123749
Mia	melanoma inhibitory activity	2.01224043	3.96002E-06	0.000670681
Cfap54	cilia and flagella associated protein 54	1.985234815	5.07793E-09	6.2781E-06
Map3k19	mitogen-activated protein kinase kinase kinase 19	1.976962508	5.20679E-10	1.17044E-06
Opn3	opsin 3	1.971705034	7.62019E-06	0.001101898
Adamts5	a disintegrin-like and metallopeptidase (reprolysin type) with thrombospondin type 1 motif, 5 (aggrecanase-2)	1.968009641	1.54179E-05	0.001945092
Nts	neurotensin	1.949119407	2.51121E-05	0.002845482
Lbp	lipopolysaccharide binding protein	1.943669204	2.11451E-10	7.10194E-07
Lrrc74b	leucine rich repeat containing 74B	1.921331387	3.46251E-09	5.03632E-06
Chml	choroideremia-like	1.884482756	0.000738683	0.039365128
Prokr2	prokineticin receptor 2	1.860870924	3.40525E-05	0.003598356
Enkur	enkurin, TRPC channel interacting protein	1.835667014	3.98856E-08	2.40549E-05

Igfbp4	insulin-like growth factor binding protein 4	1.831089736	1.39571E-05	0.001806893
Sntn	sentan, cilia apical structure protein	1.796896387	2.52425E-07	9.316E-05
Rgs22	regulator of G-protein signalling 22	1.782608924	4.99969E-08	2.80971E-05
Dnah6	dynein, axonemal, heavy chain 6	1.756719769	3.97515E-10	9.82934E-07
Lamb1	laminin B1	1.754209378	0.000334132	0.021404355
Syt10	synaptotagmin X	1.74533391	1.56527E-06	0.000317249
Gstm1	glutathione S-transferase, mu 1	1.731149158	0.000176385	0.012865711
Cd24a	CD24a antigen	1.72205109	7.52285E-05	0.006700962
Prelp	proline arginine-rich end leucine-rich repeat	1.71382009	1.17643E-08	1.07739E-05
Lgr5	leucine rich repeat containing G protein coupled receptor 5	1.708458201	3.90722E-05	0.004016764
Bbox1	butyrobetaine (gamma), 2-oxoglutarate dioxygenase 1 (gamma-butyrobetaine hydroxylase)	1.706245686	1.73325E-06	0.000345629
Gm5454	predicted gene 5454	1.699356496	6.95538E-05	0.006346335
Vwa3a	von Willebrand factor A domain containing 3A	1.696487759	1.58107E-11	3.90951E-07
Pltp	phospholipid transfer protein	1.682709556	4.95109E-11	6.12128E-07
Dnah12	dynein, axonemal, heavy chain 12	1.643619278	4.84955E-07	0.000148806
Cdhr3	cadherin-related family member 3	1.634328303	6.51363E-08	3.57917E-05
Pde3a	phosphodiesterase 3A, cGMP inhibited	1.625319394	0.000132659	0.010556302
Rgag1	retrotransposon gag domain containing 1	1.617160076	5.6123E-06	0.000883919
Chrm2	cholinergic receptor, muscarinic 2, cardiac	1.614567218	0.000235397	0.015903454
Rgs4	regulator of G-protein signaling 4	1.603924485	0.000161674	0.012005112
Crym	crystallin, mu	1.601238709	2.27187E-08	1.5595E-05
Txnip	thioredoxin interacting protein	1.593917298	0.000109381	0.008985619
Morn5	MORN repeat containing 5	1.583991106	2.07091E-06	0.000390897
Efcab1	EF hand calcium binding domain 1	1.581321917	7.49029E-09	7.71718E-06
Cdhr4	cadherin-related family member 4	1.554468998	7.35038E-10	1.29824E-06
C230072F16Rik	RIKEN cDNA C230072F16 gene	1.539775628	8.30996E-08	4.19348E-05
Lrrc55	leucine rich repeat containing 55	1.534333858	0.000156858	0.011833415
Got1l1	glutamic-oxaloacetic transaminase 1-like 1	1.529240339	4.93474E-07	0.000148806
Lrrc9	leucine rich repeat containing 9	1.496539331	1.80354E-08	1.3514E-05
LOC101056100	centrin-4 pseudogene	1.479070135	0.000171252	0.012678318
Ppil6	peptidylprolyl isomerase (cyclophilin)-like 6	1.467128769	1.05247E-05	0.001444203
Cep112it	centrosomal protein 112, intronic transcript	1.440937946	3.36403E-05	0.003585216
Gpr88	G-protein coupled receptor 88	1.428108568	7.18528E-05	0.006515021
Ccdc108	coiled-coil domain containing 108	1.426540511	5.83203E-10	1.18267E-06
Nme5	NME/NM23 family member 5	1.419790346	7.51897E-05	0.006700962
Ppp1r36	protein phosphatase 1, regulatory subunit 36	1.418404312	4.92346E-07	0.000148806
Maats1	MYCBP-associated, testis expressed 1	1.416651936	1.24334E-08	1.098E-05
St18	suppression of tumorigenicity 18	1.403115189	0.000345006	0.021930524

Mlc1	megalencephalic leukoencephalopathy with subcortical cysts 1 homolog (human)	1.398115173	0.000361453	0.022845308
Cfap44	cilia and flagella associated protein 44	1.397481609	1.93645E-07	7.72299E-05
Epha4	Eph receptor A4	1.393577679	7.63603E-05	0.006700962
Dgkk	diacylglycerol kinase kappa	1.37657437	2.50059E-05	0.002845482
Kcnmb1	potassium large conductance calcium-activated channel, subfamily M, beta member 1	1.37601288	6.5933E-09	7.41057E-06
Wdr63	WD repeat domain 63	1.370316146	6.71603E-07	0.000183907
Gna14	guanine nucleotide binding protein, alpha 14	1.364743404	2.09184E-05	0.002430373
1110017D15Rik	RIKEN cDNA 1110017D15 gene	1.347124017	3.17688E-07	0.000113848
Tekt1	tektin 1	1.343471839	1.88518E-07	7.64177E-05
Hydin	HYDIN, axonemal central pair apparatus protein	1.341877211	3.13701E-10	8.61875E-07
Rapgef5	Rap guanine nucleotide exchange factor (GEF) 5	1.34159973	0.000263903	0.017447916
Vim	vimentin	1.337070681	2.01399E-05	0.002417474
Nnat	neuronatin	1.333693624	9.1759E-07	0.000216088
Gfra2	glial cell line derived neurotrophic factor family receptor alpha 2	1.332457232	7.59939E-05	0.006700962
Ifitm3	interferon induced transmembrane protein 3	1.332103315	5.23762E-05	0.005087135
Iqcg	IQ motif containing G	1.312859737	1.56405E-06	0.000317249
Ndst4	N-deacetylase/N-sulfotransferase (heparin glucosaminyl) 4	1.30099862	0.000791012	0.041615621
Spef2	sperm flagellar 2	1.292491519	2.39479E-07	8.97212E-05
Gal	galanin	1.287194052	5.91401E-05	0.005560297
Mir490	microRNA 490	1.259595738	0.00043802	0.026849544
Mir694	microRNA 694	1.249484638	3.35986E-05	0.003585216
Dthd1	death domain containing 1	1.236425864	2.3912E-08	1.5595E-05
Cdkl4	cyclin-dependent kinase-like 4	1.222115921	2.60907E-05	0.002919203
Pdyn	prodynorphin	1.21649221	2.06162E-05	0.002430373
Ppp1r1b	protein phosphatase 1, regulatory (inhibitor) subunit 1B	1.20980565	4.80164E-07	0.000148806
Lrrc23	leucine rich repeat containing 23	1.208112209	3.60718E-07	0.000122185
Ak7	adenylate kinase 7	1.191002766	1.20061E-06	0.000258152
Zbbx	zinc finger, B-box domain containing	1.186154244	2.99882E-06	0.000525899
Gm11992	predicted gene 11992	1.177693091	1.23098E-06	0.000260157
Dynlrb2	dynein light chain roadblock-type 2	1.17076068	7.5418E-05	0.006700962
Crygn	crystallin, gamma N	1.168615618	3.58065E-06	0.000610611
Pgr15l	G protein-coupled receptor 15-like	1.157873908	9.75806E-05	0.008207063
Ccdc113	coiled-coil domain containing 113	1.157871165	7.41583E-07	0.000187113
Ccdc81	coiled-coil domain containing 81	1.156049021	3.41658E-07	0.000119022
Mdh1b	malate dehydrogenase 1B, NAD (soluble)	1.155822586	3.37334E-06	0.000579255
Csrp2	cysteine and glycine-rich protein 2	1.133319488	8.78409E-05	0.007515713
Daw1	dynein assembly factor with WDR repeat domains 1	1.132106508	8.3683E-06	0.001175699
Stoml3	stomatin (Epb7.2)-like 3	1.128378962	1.43385E-05	0.001846604

Acta2	actin, alpha 2, smooth muscle, aorta	1.122899827	0.000132657	0.010556302
Mlf1	myeloid leukemia factor 1	1.119931149	5.66853E-06	0.000887126
Iqca	IQ motif containing with AAA domain	1.107331609	1.15014E-08	1.07739E-05
Hs3st2	heparan sulfate (glucosamine) 3-O-sulfotransferase 2	1.103482621	0.00010505	0.008746026
Cfap61	cilia and flagella associated protein 61	1.086536622	1.81204E-07	7.46772E-05
Spag6l	sperm associated antigen 6-like	1.075201645	1.1786E-06	0.000256895
Wfs1	Wolfram syndrome 1 homolog (human)	1.073464837	3.88988E-07	0.000128247
AW551984	expressed sequence AW551984	1.072513954	5.20423E-06	0.000832058
Drc7	dynein regulatory complex subunit 7	1.07103701	7.75896E-07	0.000193794
Rgs9	regulator of G-protein signaling 9	1.066218308	7.35181E-05	0.00661048
Nt5dc2	5'-nucleotidase domain containing 2	1.065501488	5.65007E-05	0.005352845
Iqub	IQ motif and ubiquitin domain containing	1.058461866	0.00017327	0.012713514
Fxyd1	FXYD domain-containing ion transport regulator 1	1.056709932	5.49607E-06	0.000871163
Dmkn	dermokine	1.043487455	2.35849E-07	8.97212E-05
Adora2a	adenosine A2a receptor	1.028416318	1.56593E-05	0.001965526
Dnah9	dynein, axonemal, heavy chain 9	1.02527626	1.51741E-07	6.58262E-05
Fbxl13	F-box and leucine-rich repeat protein 13	1.023732853	6.52764E-07	0.000183907
Cfap161	cilia and flagella associated protein 161	1.020454891	9.77943E-08	4.56256E-05
Lrguk	leucine-rich repeats and guanylate kinase domain containing	1.017039065	9.68514E-07	0.000223817
Ddo	D-aspartate oxidase	1.007590312	4.12988E-06	0.000689996
Dnali1	dynein, axonemal, light intermediate polypeptide 1	1.006692459	9.09505E-07	0.000216088
Sv2c	synaptic vesicle glycoprotein 2c	-1.006974805	4.76308E-05	0.004729983
Ubash3b	ubiquitin associated and SH3 domain containing, B	-1.025783257	0.000200123	0.014058045
Egfem1	EGF-like and EMI domain containing 1	-1.036743744	0.000176957	0.012869476
Lrp1b	low density lipoprotein-related protein 1B (deleted in tumors)	-1.066548596	6.9944E-06	0.001041871
St3gal1	ST3 beta-galactoside alpha-2,3-sialyltransferase 1	-1.067651088	0.000227847	0.015649898
Cp	ceruloplasmin	-1.072897751	0.000473546	0.028420792
Cd34	CD34 antigen	-1.096428963	0.000678699	0.036743541
Frem1	Fras1 related extracellular matrix protein 1	-1.122038838	6.20896E-05	0.005770776
Nov	nephroblastoma overexpressed gene	-1.133661845	1.47498E-08	1.21573E-05
Pnoc	prepronociceptin	-1.135871377	0.000525006	0.030473788
Pcdh20	protocadherin 20	-1.138999103	0.000160728	0.011972784
Bmp3	bone morphogenetic protein 3	-1.156407183	2.27664E-06	0.000423548
Gldn	gliomedin	-1.157179382	0.000172717	0.012710652
Gm6557	predicted gene 6557	-1.181277108	4.14869E-07	0.000134521

Cck	cholecystokinin	-1.211837456	1.08186E-05	0.001469849
Car10	carbonic anhydrase 10	-1.227245133	0.000592	0.033193638
Kctd16	potassium channel tetramerisation domain containing 16	-1.228007559	0.000181932	0.013043063
Nr2f1	nuclear receptor subfamily 2, group F, member 1	-1.240152126	1.43402E-06	0.000297975
Nr2e1	nuclear receptor subfamily 2, group E, member 1	-1.251174822	0.000102511	0.008592492
Slc44a5	solute carrier family 44, member 5	-1.257333119	0.000178655	0.012954863
Chrna4	cholinergic receptor, nicotinic, alpha polypeptide 4	-1.26399561	0.000106741	0.008797922
Asic4	acid-sensing (proton-gated) ion channel family member 4	-1.272063785	0.000205736	0.014308088
Yjefn3	YjeF N-terminal domain containing 3	-1.273696342	0.00013277	0.010556302
Lamp5	lysosomal-associated membrane protein family, member 5	-1.289603284	2.96531E-06	0.000523737
Npas1	neuronal PAS domain protein 1	-1.293421516	0.000283628	0.018702021
Gm6551	predicted gene 6551	-1.298758645	1.13806E-05	0.001537751
Hrh2	histamine receptor H2	-1.307573719	0.000564437	0.032232886
Sorcs3	sortilin-related VPS10 domain containing receptor 3	-1.406597317	0.000420068	0.025838336
Nrn1	neuritin 1	-1.473745744	0.000546249	0.031338954
Nt5dc3	5'-nucleotidase domain containing 3	-1.508259701	0.000305552	0.019830428
Krt73	keratin 73	-1.5265264	3.09913E-05	0.003351854
Chrna7	cholinergic receptor, nicotinic, alpha polypeptide 7	-1.545668968	0.000222884	0.015394532
Rgs12	regulator of G-protein signaling 12	-1.585615266	3.96382E-05	0.004050141
Npas3	neuronal PAS domain protein 3	-1.644821513	4.16168E-05	0.004217458
Sel1l3	sel-1 suppressor of lin-12-like 3 (C. elegans)	-1.65833421	1.24773E-05	0.001649874
Slc17a8	solute carrier family 17 (sodium-dependent inorganic phosphate cotransporter), member 8	-1.699947295	4.18899E-07	0.000134521
Car4	carbonic anhydrase 4	-1.731523231	5.21571E-06	0.000832058
Cadps2	Ca2+-dependent activator protein for secretion 2	-1.761320975	0.00022964	0.015685902
Atp6ap1l	ATPase, H+ transporting, lysosomal accessory protein 1-like	-1.814603939	1.54183E-09	2.54166E-06
Chrna5	cholinergic receptor, nicotinic, alpha polypeptide 5	-1.990173854	0.000160754	0.011972784
Htr3a	5-hydroxytryptamine (serotonin) receptor 3A	-2.142378624	0.000454411	0.02740539
Grpr	gastrin releasing peptide receptor	-2.176458102	0.000568115	0.032366955
Pde11a	phosphodiesterase 11A	-2.230899307	4.33174E-09	5.63742E-06

Crh	corticotropin releasing hormone	-2.434900902	0.000183036	0.013043063
Tac2	tachykinin 2	-2.44478717	2.7253E-05	0.003035514
Cdh9	cadherin 9	-2.487432457	0.00015037	0.011560622
Sema3c	sema domain, immunoglobulin domain (Ig), short basic domain, secreted, (semaphorin) 3C	-2.540710349	7.81641E-06	0.001123699
Zfp804b	zinc finger protein 804B	-2.592425923	2.20456E-05	0.002523709
Egln3	egl-9 family hypoxia-inducible factor 3	-2.610491382	2.33779E-06	0.000428196
Nr2f2	nuclear receptor subfamily 2, group F, member 2	-2.628341112	1.58659E-05	0.001981398
Npy1r	neuropeptide Y receptor Y1	-2.67519904	2.81605E-05	0.003108597
Ndnf	neuron-derived neurotrophic factor	-2.686352007	2.29771E-10	7.10194E-07
Reln	reelin	-2.759418778	8.14289E-08	4.19348E-05
Rxfp1	relaxin/insulin-like family peptide receptor 1	-2.967544009	8.59091E-07	0.000210324
Tnfaip8l3	tumor necrosis factor, alpha-induced protein 8-like 3	-3.119866547	3.10387E-07	0.000112867
Adarb2	adenosine deaminase, RNA-specific, B2	-3.267996658	8.02675E-08	4.19348E-05
Cxcl14	chemokine (C-X-C motif) ligand 14	-3.514920601	2.04843E-08	1.44719E-05
Vip	vasoactive intestinal polypeptide	-4.895220551	5.09932E-07	0.000151917

Supplementary Table 4. Signalling pathway impact analysis (SPIA) calculated after striatum vs. cortex (ST/CTX) DE genes from the *PV-CRE; tdTomato* mice.

Pathway	**ID**	**KEGG *P* Value**	**tA**	**Perturbation *P* Value**	***P* Value**	**FDR**
Central carbon metabolism in cancer	05230	0.16392	23.931	0.008	0.01001	0.32625
GnRH signaling pathway	04912	0.63447	23.036	0.007	0.02849	0.32625
PI3K-Akt signaling pathway	04151	0.09786	15.537	0.085	0.04815	0.32625
FoxO signaling pathway	04068	0.06831	9.977	0.065	0.02849	0.32625
Focal adhesion	04510	0.00232	9.592	0.295	0.00568	0.32625
Small cell lung cancer	05222	0.07223	8.194	0.104	0.04425	0.32625
Dorso-ventral axis formation	04320	0.26739	3.290	0.003	0.00652	0.32625
Retrograde endocannabinoid signaling	04723	0.10912	2.624	0.064	0.04165	0.32625
Huntington's disease	05016	0.00161	0	1	0.01200	0.32625
Morphine addiction	05032	0.02018	-1.146	0.301	0.03707	0.32625
Thyroid cancer	05216	0.27611	-1.200	0.026	0.04261	0.32625
Complement and coagulation cascades	04610	0.00347	-1.216	0.772	0.01855	0.32625
Colorectal cancer	05210	0.51253	-1.600	0.011	0.03483	0.32625
cAMP signaling pathway	04024	0.00764	-4.825	0.281	0.01533	0.32625
Apelin signaling pathway	04371	0.44296	-8.121	0.007	0.02101	0.32625

Supplementary Table 5. Signalling pathway impact analysis (SPIA) calculated after striatum vs. cortex (ST/CTX) DE genes from the *PV-tdTomato* mice.

Pathway	**ID**	**KEGG *P* Value**	**tA**	**Perturbation *P* Value**	***P* Value**	**FDR**
Calcium signaling pathway	04020	8.65E-05	6.356	0.269	0.00027	0.00747
cAMP signaling pathway	04024	0.0044	1.830	0.724	0.02135	0.23492
Alcoholism	05034	0.00541	0.357	0.941	0.03197	0.29314
Cocaine addiction	05030	0.00055	-4.306	0.155	0.00088	0.01630
Long-term depression	04730	0.36428	-7.305	0.023	0.04844	0.38064
Cholinergic synapse	04725	0.05675	-10.293	0.053	0.02047	0.23492